Analysis, Modeling and Simulation of Multiscale Problems

Repulsive interaction of Néel walls, and the internal length scale of the cross–tie wall

Antonio DeSimone, Robert V. Kohn, Stefan Müller & Felix Otto

Preprint 32

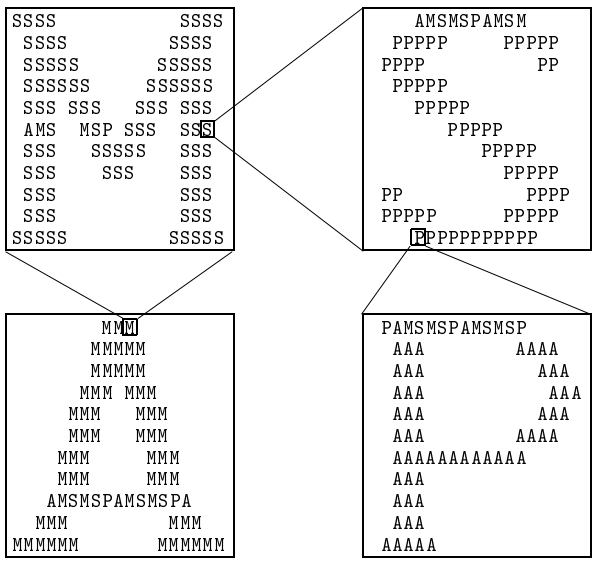

Schwerpunktprogramm der Deutschen Forschungsgemeinschaft

Repulsive interaction of Néel walls, and the internal length scale of the cross–tie wall

Antonio DeSimone[*], Robert V. Kohn[†], Stefan Müller[‡], Felix Otto[§]

February 19, 2002

Abstract

Néel walls and cross–tie walls are two structures commonly seen in ferromagnetic thin films. They are interesting because their internal length scales are not determined by dimensional analysis alone. This paper studies (a) the repulsive interaction of one–dimensional Néel walls; and (b) the internal length scale of the cross–tie wall. Our analysis of (a) is mathematically rigorous; it provides, roughly speaking, the first two terms of an asymptotic expansion for the energy of a pair of interacting walls. Our analysis of (b) is heuristic, since it rests on an analogy between the cross–tie wall and an ensemble of Néel walls. This analogy, combined with our results on Néel walls and a judicous choice of parameter regime, yields a specific prediction for the internal length scale of a cross–tie wall. This prediction is consistent with the experimentally–observed trends.

Contents

[*]Max–Planck–Institut für Mathematik in den Naturwissenschaften, Leipzig, Germany, and Dip. Ingegneria Civile e Ambientale Politecnico di Bari, Italy, desimone@mis.mpg.de

[†]Courant Institute of Mathematical Sciences, New York University, USA, kohn@cims.nyu.edu

[‡]Max–Planck–Institut für Mathematik in den Naturwissenschaften, Leipzig, Germany, sm@mis.mpg.de

[§]Institut für Angewandte Mathematik, Universität Bonn, Germany, otto@iam.uni-bonn.de

1 Introduction

The Néel wall is a dominant wall type in soft thin magnetic films. Unlike most transition layers in materials science, Néel walls have extremely slowly (logarithmically) decaying tails. These tails are confined only by anisotropy, by the sample edges, or by the tails of neighboring Néel walls. If the confining mechanism comes from the tails of neighboring walls (which cannot unwind and thus annihilate themselves) then there is a strong repulsive interaction between the walls.

The cross–tie wall is another typical pattern seen in soft thin films. It resembles an ensemble of Néel walls, with a characteristic pattern and a well–defined internal length scale w_{cross}. Experimentally w_{cross} is known to decrease as the film thickness increases. It also decreases as the material anisotropy increases. There is however no accepted theory predicting the value of w_{cross} or even the experimentally observed trends.

The origin of this paper is the observation that these two problems are related. Indeed, if the cross–tie wall resembles an ensemble of Néel walls, then its internal length scale should be determined by the repulsive interaction of Néel wall tails. We are thus led to explore both (a) the interaction of Néel walls, and (b) the internal length scale of a cross–tie wall.

The complexity and multiscale character of thin–film micromagnetics makes it particularly fruitful to consider these topics simultaneously. There are three distinct length scales — the exchange length d, the film thickness t, and the wall spacing w. So there are two nondimensional parameters, and a multitude of possible regimes. The application to cross–tie walls will guide our attention to a specific parameter regime, namely

$$d \ll w \quad \textit{and} \quad \ln \frac{w}{d} \ll \frac{t}{d} \ll \frac{w}{d},$$

as the one that is relevant to cross–tie walls.

This paper presents a mixture of rigorous and heuristic argument. Our results on one–dimensional Néel walls are fully rigorous. Our deductions concerning cross–tie walls are heuristic, since they depend on the caricature of a cross–tie wall as

an ensemble of Néel walls. Such a mixture of rigor and heuristics may be unusual, however it seems to us quite natural. The heuristic arguments identify the "essential physics" determining the length scale of a cross–tie wall; the rigorous arguments analyse the consequences of the essential physics, in the simplest possible setting.

The analysis of Néel walls has interest far beyond the specific application emphasized here, to cross–tie walls. Indeed, the interaction of such walls with one another or with the boundary of a sample creates significant energy barriers. This effect grows stronger with decreasing film thickness t. It can be responsible for the inaccessibility of energetically favorable states, and thus is one source of magnetic hysteresis in soft thin ferromagnetic films. An example of such hysteresis — involving repulsive interaction of a wall with a sample boundary — is discussed in [3].

The analysis of one–dimensional Néel walls also has considerable mathematical interest. The problem is challenging because it amounts to a nonlocal, nonconvex variational problem with a small parameter. Our approach is to prove matching upper and lower bounds on the minimum energy. Finding a good upper bound is more or less routine: it suffices to minimize the energy within a suitable ansatz. Finding a matching lower bound is much less routine; it is the heart of our mathematical achievement.

The rest of this introduction summarizes briefly the structure of the paper. Section 2 reviews the basic micromagnetic model, first discussing the fully three–dimensional problem (Subsection 2.1), then making the reduction to magnetization independent of x_3 (Subsection 2.2).

Section 3 introduces Néel walls and cross–tie walls, and discusses the relation between them. We start, in Subsection 3.1, with the definition of a one–dimensional Néel wall. Then, in Subsection 3.2, we discuss how to quantify the repulsion between Néel walls; in particular, we define the repulsive force $\mu(d, t, w)$ between winding Néel walls at distance w. Then we turn, in Subsection 3.3, to cross–tie walls, reviewing their basic features and explaining the relevance of μ. We show, in particular, that to account for the experimentally–observed trends, μ should have certain scaling behavior in w and t (mainly: μ should grow sublinearly in t).

Section 4 formulates and discusses our rigorous results on one–dimensional Néel walls. The subtlety of this problem arises because the magnetostatic term displays a cross–over between two homogeneous expressions, associated with the thick–film ($t/w \to \infty$) and thin–film ($t/w \to 0$) limits respectively. Subsection 4.1 considers the "thick–film regime," i.e. the variational problem obtained by replacing the magnetostatic term with its limiting behavior as $t/w \to \infty$. Subsection 4.2 considers the opposite "thin–film regime," obtained by replacing the magnetostatic term with its limiting expression as $t/w \to 0$. As we shall see, neither limiting regime gives the desired behavior for μ! Therefore in Subsection 4.3 we consider the original variational problem, with the full magnetostatic term, and we identify an "intermediate regime" in which μ does indeed have the expected behavior.

Section 5 contains the proofs of our results on one–dimensional Néel walls. The thick–film regime, analyzed in Subsection 5.1, is relatively easy. The thin–film regime, analyzed in Subsection 5.2, is relatively long and technical. Readers primarily interested in cross–tie walls may however skip Subsection 5.2, proceeding directly to Subsection 5.3. It gives the proof of our main result, Theorem 1, evaluating the optimal energy in the intermediate regime associated with cross–tie walls.

2 Ferromagnetic thin films

2.1 Three dimensional micromagnetics

The micromagnetic model states that the experimentally observed ground state for the magnetization m is a minimizer of the following variational problem.

We consider a ferromagnetic sample in form of a film of thickness t in x_3–direction and of infinite lateral size, i. e.

$$\mathbb{R}^2 \times (-\frac{t}{2}, \frac{t}{2}).$$

We call a magnetization $m\colon \mathbb{R}^2 \times (-\frac{t}{2}, \frac{t}{2}) \to \mathbb{R}^3$ admissible if it has unity spontaneous magnetization

$$|m|^2 \;=\; 1 \quad \text{in } \mathbb{R}^2 \times (-\frac{t}{2}, \frac{t}{2}) \tag{1}$$

and is periodic in x_1 and x_2–directions with period $2\,w$

$$\begin{aligned} m(x_1 + 2\,w, x_2, x_3) &= m(x_1, x_2, x_3), \\ m(x_1, x_2 + 2\,w, x_3) &= m(x_1, x_2, x_3). \end{aligned}$$

The motivation for the periodicity assumption will be given in Subsection 3.2.

The micromagnetic energy per (lateral) periodic cell is given by

$$\begin{aligned} E_{3d}(m) \;=\; & d^2 \int_{(-w,w)^2 \times (-\frac{t}{2}, \frac{t}{2})} |\nabla m|^2 \, dx + \int_{(-w,w)^2 \times \boldsymbol{R}} |\nabla u|^2 \, dx \\ & + Q \int_{(-w,w)^2 \times (-\frac{t}{2}, \frac{t}{2})} (m_1^2 + m_3^2) \, dx, \end{aligned} \tag{2}$$

where the potential u, which is supposed to inherit the symmetries of m, i. e.

$$\begin{aligned} u(x_1 + 2\,w, x_2, x_3) &= u(x_1, x_2, x_3), \\ u(x_1, x_2 + 2\,w, x_3) &= u(x_1, x_2, x_3), \end{aligned}$$

is determined by the static Maxwell equations, which we formulate variationally:

$$\int_{R^3} \nabla u \cdot \nabla \zeta \, dx \;=\; \int_{\boldsymbol{R}^2 \times (-\frac{t}{2}, \frac{t}{2})} m \cdot \nabla \zeta \, dx \quad \text{for all } \zeta \in C_0^\infty(\mathbb{R}^3). \tag{3}$$

The first term in (2) is the so–called exchange energy, the second term is the energy of the stray field $H_{str} = -\nabla u$. The third term comes from crystalline anisotropy which favors a certain magnetization axis, say, the m_2–axis. The nondimensional parameter Q is called the quality factor.

The classical formulation of (3) is

$$\left.\begin{array}{rcl} \nabla^2 u & = & \left\{\begin{array}{ll} \nabla\cdot m & \text{in } \mathbb{R}^2\times(-\frac{t}{2},\frac{t}{2}) \\ 0 & \text{in } \mathbb{R}^2\times[(-\infty,-\frac{t}{2})\cup(\frac{t}{2},+\infty)] \end{array}\right\} \\ [u] & = & 0 \quad \text{and} \quad \left[\frac{\partial u}{\partial x_3}\right] = \mp m_3 \quad \text{on } \mathbb{R}^2\times\{\pm\frac{t}{2}\} \end{array}\right\}, \tag{4}$$

where $[\cdot]$ denotes the jump of quantity $\cdot$ across the boundary of the sample. We gather from (4) that there are two sources of stray field. By electrostatic analogy, one speaks of volume and surface "charges":

$$\begin{array}{lll} \text{volume charge density:} & -\nabla\cdot m & \text{in } \mathbb{R}^2\times(-\frac{t}{2},\frac{t}{2}), \\ \text{surface charge density:} & \pm m_3 & \text{on } \mathbb{R}^2\times\{\pm\frac{t}{2}\}. \end{array}$$

This model is already partially non–dimensionalized: The magnetization m, the field $H_{str} = -\nabla u$, and the energy density are dimensionless. However, length is still dimensional. In fact, there are four length scales: two intrinsic scales (i.e. only depending on the material) and two extrinsic scales (i.e. only depending on the sample geometry):

$$\begin{array}{ll} \text{intrinsic scales:} & d \text{ and } d/Q^{\frac{1}{2}}, \\ \text{extrinsic scales:} & t \text{ and } w. \end{array} \tag{5}$$

The functional (2) is positive quadratic. It is the constraint (1) which makes the variational problem a *nonconvex* one. The magnetostatic energy in (2) makes it a *nonlocal* variational problem in m, since the energy density depends in a nonlocal way on the order parameter m, namely through the equation (3) which determines the potential u. The *multiscale* nature (5) of the variational problem, together with its nonconvexity and nonlocality, leads to a rich behavior and pattern formation on intermediate scales.

2.2 Two–dimensional reduction

In sufficiently thin films, it seems reasonable to assume that the magnetization is essentially independent of the thickness direction x_3:

$$m = m(x'), \tag{6}$$

where throughout the text, the prime indicates the in–plane components 1 and 2. The right measure of film thickness is the ratio $\frac{t}{d}$. In fact, (6) approximately holds for not too thick films, up to $\frac{t}{d} \approx 20$ for Permalloy ($Q = 0.00025$), see [7, Fig.3.79]. For thicker films, a wall type which violates (6) is observed. This so–called asymmetric Bloch wall is nicely explained in [7, 3.6.4(D)] but will not be treated here.

For magnetizations with (6), the penalization of volume charges and surface charges

$$\begin{array}{lllll} \text{volume charge density:} & -\nabla' \cdot m' & \text{in} & I\!R^2 \times (-\frac{t}{2}, \frac{t}{2}), \\ \text{surface charge density:} & \pm m_3 & \text{on} & I\!R^2 \times \{\pm\frac{t}{2}\} \end{array}$$

separates. This can be best seen by passing to Fourier series of the $(-w, w)^2$–periodic vector field $m\colon I\!R^2 \to I\!R^3$, i. e.

$$m_{j,n'} \;=\; \frac{1}{2\,w} \int_{(-w,w)^2} e^{i\,\pi\,\frac{n'}{w}\cdot x'}\, m_j(x')\, dx' \quad \text{for } n' \in Z\!\!\!Z^2.$$

We write $m'_{n'} = (m_{1,n'}, m_{2,n'})$. Indeed, we have

$$\int_{(-w,w)^2\times \boldsymbol{R}} |\nabla u|^2\, dx \;=\; t \sum_{n'} f\left(\frac{\pi\,|n'|\,t}{2\,w}\right) \left|\frac{n'}{|n'|}\cdot m'_{n'}\right|^2 + t \sum_{n'} g\left(\frac{\pi\,|n'|\,t}{2\,w}\right) |m_{3,n'}|^2,$$

where the Fourier multipliers are given by

$$g(z) \;=\; \frac{\sinh(z)}{z\,\exp(z)} \quad \text{and} \quad f(z) \;=\; 1 - g(z). \tag{7}$$

This Fourier representation of the stray field energy is obtained as follows: The Fourier transform of (4) in the horizontal variables yields an ordinary differential equation in x_3 with ξ' as parameter and with piecewise constant r. h. s. . This ode can be solved explicitly. The formula then follows from Plancherel's identity in the horizontal variables. We observe that the Fourier multipliers display a *cross–over*:

$$f(z) \;\approx\; \left\{ \begin{array}{ll} z & \text{for } z \ll 1 \\ 1 & \text{for } z \gg 1 \end{array} \right\} \quad \text{and} \quad g(z) \;\approx\; \left\{ \begin{array}{ll} 1 & \text{for } z \ll 1 \\ \frac{1}{2\,z} & \text{for } z \gg 1 \end{array} \right\}. \tag{8}$$

Hence the way charge densities are penalized depends on the characteristic length scale ℓ over which they vary. In terms of the length scale ℓ, this cross–over is of the order of the film thickness t. Hence for sufficiently thin films, it seems reasonable to replace $f(z)$ by z, whereas for sufficiently thick films, it seems plausible to replace $f(z)$ by 1. This cross–over will play an important role in our analysis.

Summing up: Under the assumption (6), we obtain the functional

$$\begin{aligned} E_{2d}(m) \;=\;& d^2\, t \int_{(-w,w)^2} |\nabla' m|^2\, dx' \;+\; Q\, t \int_{(-w,w)^2} (m_1^2 + m_3^2)\, dx' \\ & + t \sum_{n'} f\left(\frac{\pi\,|n'|\,t}{2\,w}\right) \left|\frac{n'}{|n'|}\cdot m'_{n'}\right|^2 \;+\; t \sum_{n'} g\left(\frac{\pi\,|n'|\,t}{2\,w}\right) |m_{3,n'}|^2, \end{aligned} \tag{9}$$

which is to be minimized among all $m\colon I\!R^2 \to I\!R^3$ with

$$m(x_1 + 2\,w, x_2) \;=\; m(x_1, x_2) \quad \text{and} \quad m(x_1, x_2 + 2\,w) \;=\; m(x_1, x_2)$$

under the constraint

$$|m|^2 \;=\; 1 \quad \text{on } I\!R^2.$$

3 Néel walls and cross-tie walls

3.1 The one–dimensional Néel wall

A wall is a transition layer which connects two essentially constant magnetizations $m^{\pm}$. In a soft thin film, walls are commonly of Néel type. The simplest model of such a wall assumes that m depends only on the transverse variable, i.e.

$$m \;=\; m(x_1).$$

Contrary to the Bloch wall in bulk samples (see [7, 3.6.1(A)]), the Néel wall avoids surface charges at the expense of volume charges. It achieves this by an entirely in–plane rotation

$$m_3 \;=\; 0.$$

Hence we may describe a Néel wall by the angle θ the magnetization forms with the wall normal

$$m' \;=\; \begin{pmatrix} \cos\theta \\ \sin\theta \end{pmatrix}. \tag{10}$$

Figures 1 give a sketch of the magnetization within a Néel wall. The relevant energy functional is

$$E_{1d}(m') \;=\; d^2\, t \int_{-w}^{w} |\frac{dm'}{dx_1}|^2\, dx_1 + t \sum_{n_1} f\left(\frac{\pi\,|n_1|\,t}{2\,w}\right)\, |m_{1,n_1}|^2 + Q\,t \int_{-w}^{w} m_1^2\, dx_1, \tag{11}$$

where the one–dimensional Fourier coefficients are given by

$$m_{1,n_1} \;=\; \frac{1}{(2w)^{\frac{1}{2}}} \int_{-w}^{w} e^{i\,\pi\,n_1\,\frac{x_1}{w}} m_1(x_1)\, dx_1 \quad \text{for } n_1 \in \mathbb{Z}.$$

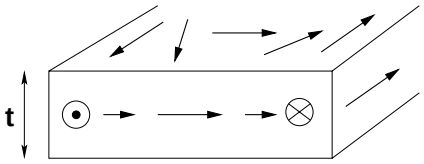

Figure 1: Magnetization in Néel wall

It is well understood from formal arguments and from numerical simulations in the physics literature that the Néel wall consists of two qualitatively distinct elements: the *core* and a slowly decaying *tail*. For the convenience of the reader, we cite the key sentences from the careful discussion in [7, 3.6.4(C)]: "Part of the charge is concentrated in the core, where it supports a low energy state by the close interaction with its counterpart of opposite polarity. This part is limited by the exchange energy, which prevents an arbitrarily narrow core width. The other part of the charge gets widely spread in the tail". As we shall see in Subsection 4.2, the larger the tail width w, the lower the stray field energy. Hence it is important that the tail is confined by some mechanism to a length w. Otherwise, the tail would take over the entire rotation of the magnetization at vanishing cost: The two bulk magnetizations $m^{\pm}$ would "diffuse" into each other.

3.2 Repulsive interaction between Néel walls

The mechanism which contains the tails of a Néel wall can be anisotropy favoring the bulk magnetizations $m^{\pm} = \binom{0}{\pm 1}$ as in (11), or it can be the finite size of the sample. In this paper, we investigate the case where the tail is confined by the tail of a neighboring wall at distance w. Hence we also neglect anisotropy and just consider

$$E_{1d}(m') \;=\; d^2\, t \int_{-w}^{w} |\frac{dm'}{dx_1}|^2\, dx_1 \;+\; t \sum_{n_1} f\left(\frac{\pi\,|n_1|\,t}{2\,w}\right)\, |m_{1,n_1}|^2. \tag{12}$$

The simplest way to realize this repulsive interaction is to consider a periodic array of winding walls of distance w. This is enforced by imposing the conditions

$$\theta(x_1 + w) \;=\; \theta(x_1) + \pi \tag{13}$$

on the magnetization angle. Observe that this entails periodicity of m' of period $2\,w$, i. e.

$$m'(x_1 + 2\,w) \;=\; m'(x_1).$$

Figure 2 and 3 show a sketch of an array of winding Néel walls and the corresponding polarity of the charge distribution. Observe that these Néel walls are 180^o Néel walls in the sense that adjacent bulk magnetizations $m^{\pm}$ differ by a rotation of 180^o.

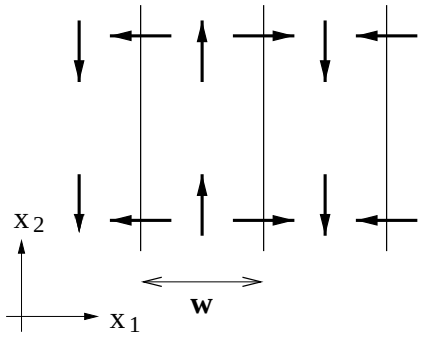

Figure 2: Magn. in winding Néel wall

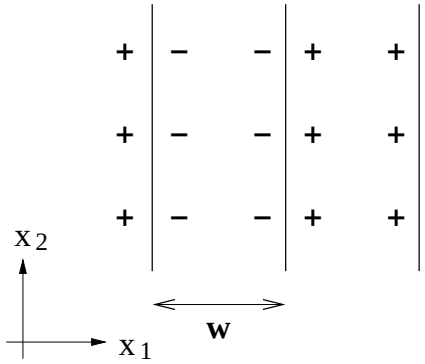

Figure 3: Charges in winding Néel wall

The goal of this paper is to quantify the repulsive force between Néel wall tails. "Winding walls ... show a repulsion which increases strongly with decreasing wall distance" [5]. Actually, a quantitative analysis of this repulsive force is still considered an open question by the physics community [7, p.245] both analytically and numerically. Let $e(d,t,w)$ denote the minimum of (12) among all magnetizations m' with (10) and (13):

$$e(d,t,w) \;:=\; \min_{m' \text{ satisfies (10) and (13)}} E_{1d}(m').$$

Observe that this is *twice* the specific Néel wall energy. The repulsive force given by

$$\mu(d,t,w) \;=\; \frac{\partial e}{\partial w}(d,t,w).$$

Hubert & Holz [6, p.148] were the first to try to quantify the increase in the specific energy of a Néel wall due to a decreasing distance w to a neighboring wall. They write "Es ist für viele Fragen von Interesse, wie die Energie der Néelwand zunimmt, wenn die Länge des Ausläufers künstlich eingeschränkt wird, etwa durch eine benachbarte Wand gleichen Drehsinns oder durch die Probenberandung. Überschlagsmäßige Rechnungen zeigen, daß die Wandenergie näherungsweise durch

$$E_g \;=\; E_{g0} + E_{g1} \left(\frac{D}{x_c}\right)^{\frac{1}{3}} \tag{14}$$

dargestellt werden kann."[1] In our notation, (14) turns into

$$\frac{1}{d\,t}\, e(d,t,w) \;=\; e_0(\frac{t}{d}) + e_1(\frac{t}{d}) \left(\frac{t}{w}\right)^{\frac{1}{3}}. \tag{15}$$

We have been unable to identify a regime where (15) holds.

3.3 Cross–tie walls

We are in particular interested how the force μ depends on thickness t, since this helps to understand the cross–tie wall, as we shall see. The cross–tie wall, c.f. [7, 3.6.4], is a pattern consisting of a main Néel wall segment and perpendicular short Néel wall segments (the "cross–ties"), see Figure 4, which shows a schematic pattern of the cross–tie wall. The main Néel wall segment is parallel to the easy axis (the axis favored by crystalline anisotropy, indicated by Q in Figure 4, which here is the m_1–axis). The cross–ties have an equilibrium period w_{cross}. It is conjectured that the relevant repulsive force which keeps these Néel walls apart — and thus sets the equilibrium period w_{cross} — comes from the fact that the length of the tails of the main wall segment are limited by the tails of the adjacent cross–ties and vice versa [7, p.245]. Figures 5 and 6 zoom in on the neighborhood of the intersection of the main wall segment with a cross–tie. They indicate the sense of rotation of the magnetization and the sign of the volume charge distribution. Observe that the average distance between the repelling Néel wall segments scales as w_{cross}.

The reason why one observes this microstructure of Néel walls instead of a single 180^o–Néel wall is actually well–understood: All Néel walls in the cross–tie pattern are of 90^o or less. It is known from numerical simulations that a 90^o–Néel wall has only approximately 12% of the specific energy of a 180^o–Néel wall in an experimentally relevant parameter regime [7, p.240]. Hence although the total length of walls in Figure 4 is larger, the total wall energy is smaller than for a single wall. Very recently, Alouges, Riviére and Serfaty identified the proportions of the optimal wall pattern in a cross–tie wall [1] (which has smooth transitions instead of the diagonal walls in Figure 4, in agreement with numerical simulations and experiments)!

[1] "It is of interest for many applications how the energy of a Néel wall increases as the length of its tail is constrained artificially, for instance through a neighboring wall of same winding sense or the sample edge. Rough calculations show that the wall energy can be approximated by ..."

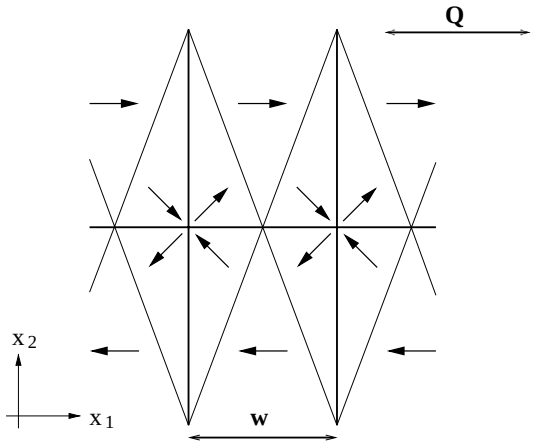

Figure 4: Magnetization in cross–tie wall

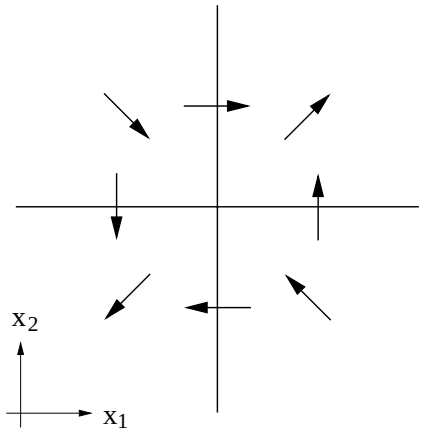

Figure 5: Magnetization near cross–tie

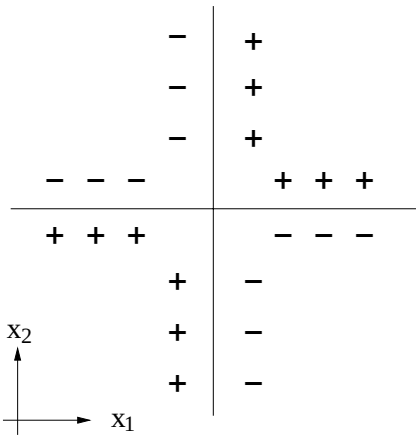

Figure 6: Volume charges near cross–tie

Roughly speaking, their starting point is the expression for the *angle–dependent* specific Néel wall energy valid in sufficiently thick films. But their analysis, though very impressive, neglects anisotropy and the repulsive interaction between the walls. Therefore it does not capture the mechanisms that determine w_{cross} — the objective of this paper.

The mechanisms which set the equilibrium cross–tie period w_{cross} are still debated: "... a consistent theory of the cross–tie wall is still lacking. Numerical computations point in the right direction but are necessarily restricted to small cross–tie periods." [7, p.245]. Experimentally, the cross–tie wall is ubiquitous and well–studied. Experiments show that the cross–ties move closer together with increasing crystalline [9, Fig 7]:

$$w_{cross} \text{ is proportional to } \frac{1}{Q}. \tag{16}$$

It is also experimentally observed that cross–ties move closer together as the film

thickness t increases [7, Fig 5.59]:

$$w_{cross} \text{ decreases as } t \text{ increases.} \tag{17}$$

There is no doubt that the force which keeps the cross–ties close together is crystalline anisotropy: In a band of a thickness which scales with w_{cross}, the magnetization deviates $O(1)$ from the easy direction, see Figure 4. In view of (9) (with easy axis m_1 instead of m_2), the anisotropy energy scales as $Q\,t\,w_{cross}$. Hence the attractive potential μ_{attr} scales as

$$\mu_{attr} \;\sim\; Q\,t \quad \text{or} \quad \frac{1}{d}\,\mu_{attr} \;\sim\; Q\,\frac{t}{d}. \tag{18}$$

In order to be compatible with (16) and (17), the repulsive potential μ_{rep} should obviously scale as

$$\frac{1}{d}\,\mu_{rep} \;\approx\; -h(\frac{t}{d})\,\frac{d}{w} \quad \text{with } \textit{sublinear } h.$$

By "sublinear" we mean $h(z) \sim z^\alpha$ with $\alpha < 1$ for $z \gg 1$ or $z \ll 1$ (either would do). If the relevant repulsive force comes indeed from the repulsion of Néel wall tails, we expect

$$\mu_{rep} \;\sim\; \mu(d, t, w_{cross}),$$

since the average distance between the winding Néel wall segments in Figure 4 scales with w_{cross}. *Hence if the hypothesis that the relevant repulsive interaction between cross-ties comes from the repulsive interaction of Néel wall tails is true, there should be a regime such that*

$$\frac{1}{d}\,\mu(d, t, w) \;\approx\; -h(\frac{t}{d})\,\frac{d}{w} \quad \text{with } \textit{sublinear } h. \tag{19}$$

Of course, this argument is purely heuristic: One of its implicit hypothesis is that the correction — at least in scaling — to the specific Néel wall energy due to confinement by neighboring Néel walls is independent of the angle of these Néel walls and also applies to more complicated geometries where the neighboring walls are not necessarily parallel at distance w, but only have average distance w. Hence the goal of this paper is to identify a parameter regime where (19) holds. In fact, in Theorem 1 we will show that

$$\frac{1}{d}\,\mu(d, t, w) \;\approx\; -4\,\pi\,\frac{d}{w} \quad \text{for} \quad d \;\ll\; w \quad \text{and} \quad \ln\frac{w}{d} \;\ll\; \frac{t}{d} \;\ll\; \frac{w}{d}.$$

Together with (18), this predicts the scaling

$$w_{cross} \;\sim\; \frac{d^2}{Q\,t} \quad \text{for} \quad Q \;\ll\; 1 \quad \text{and} \quad \ln\frac{1}{Q} \;\ll\; \frac{t}{d} \;\ll\; \frac{1}{Q^{\frac{1}{2}}}.$$

Not just the scaling but also the regime is consistent with the experimental observations for Permalloy [7, Fig 5.59].

4 Announcement and discussion of rigorous results

It seems hopeless to find an analytic expression for $\mu(d,t,w)$ or $e(d,t,w)$. The strategy therefore is asymptotic analysis: Find analytic expressions which approximate $e(d,t,w)$ in certain parameter regimes. It thus seems natural to first investigate the *homogeneous* expressions (8) for the Fourier multiplier f separately. The resulting variational problem then has a *single* non–dimensional parameter (instead of two) and therefore a much reduced complexity. They will be treated in Subsection 4.1 for the "thick–film regime", i. e.

thick–film approximation: $f(z)$ is replaced by 1

and in Subsection 4.2 for the "thin–film regime", i. e.

thin–film approximation: $f(z)$ is replaced by z.

But, as we shall see, both of these homogeneous reductions fail to capture a regime with (19)! That such an intermediate regime exists is only revealed by a more careful analysis of the true energy, which is presented in Subsection 4.3.

4.1 The thick–film regime

For sufficiently thick films, it seems justified to replace f in (12) by the second homogeneous expression in (8), so that we are led to consider

$$E_{thick}(m) \;=\; d^2\,t\,\int_{-w}^{w}|\frac{dm'}{dx_1}|^2\,dx_1 \;+\; t\,\int_{-w}^{w} m_1^2\,dx_1, \tag{20}$$

which is an entirely local functional. This allows for a standard treatment of the wall. As for E_{1d}, we denote the minimum of E_{thick} among all m' with (10) and (13) with $e_{thick}(d,t,w)$.

Proposition 1 *In the regime of sufficiently distant walls in the sense of*

$$d \;\ll\; w, \tag{21}$$

we have

$$\frac{1}{d\,t}\,e_{thick}(d,t,w) \;-\; 8 \;\approx\; 2\,\exp(-\frac{w}{d}). \tag{22}$$

(21) and (22) is just a short notation for the following statement: For any $\epsilon > 0$, there exists a $\delta > 0$ such that whenever

$$d \;\leq\; \delta\,w,$$

we have

$$1-\epsilon \;\leq\; \frac{\frac{1}{d\,t}\,e_{thick}(d,t,w) \;-\; 8}{2\,\exp(-\frac{w}{d})} \;\leq\; 1+\epsilon.$$

We shall now address two questions

A) When does the thick–film approximation seem reasonable?

B) What (tentative) predictions may we draw from Proposition 1 w. r. t. μ?

Question A). The proof of Proposition 1 indicates that the minimizer features a core of size d (with exponential decay), but no slowly decaying tail. In particular, the largest length scale is of order d. Hence the approximation of $f(z)$ by 1 is seemingly justified if and only if

$$t \gg d. \tag{23}$$

Hence we expect (22) to be a good approximation as long as (23) is satisfied. In Subsection 4.3, we shall see that even for the leading order term $E_{thick} \approx 8\, d\, t$, this is too optimistic by a logarithm.

Question B). In view of the answer to A), Proposition 1 predicts that for sufficiently thick films in the sense of (23) and for sufficiently far–away walls in the sense of (21), we have

$$\frac{1}{d}\,\mu(d,t,x) \;\approx\; \frac{1}{d}\,\mu_{thick}(d,t,x) \;\approx\; -\frac{t}{d}\,\exp(-\frac{w}{d}). \tag{24}$$

Thus we obtain an exponential dependence on w instead of the desired inverse proportionality in (19). In fact, this tentative prediction is wrong (apart from the regime of extremely thick films), as we shall see in Subsection 4.3!

4.2 The thin–film regime

For sufficiently thin films, it seems justified to replace to replace f in (12) by the first homogeneous expression in (8), so that we are lead to consider

$$E_{thin}(m) \;=\; d^2\, t \int_{-w}^{w} |\frac{dm'}{dx_1}|^2\, dx_1 \;+\; t^2 \sum_{n_1} \frac{\pi\, |n_1|}{2\, w}\, |m_{1,n_1}|^2. \tag{25}$$

As for E_{1d}, we denote the minimum of E_{thin} among all m' with (10) and (13) with $e_{thin}(d,t,w)$.

Proposition 2 *In the regime of sufficiently distant walls in the sense of*

$$\frac{d^2}{t} \;\ll\; w, \tag{26}$$

we have

$$\frac{\ln \frac{w\,t}{d^2}}{t^2}\, e_{thin}(d,t,w) \;-\; \pi \;\sim\; \frac{\ln\ln \frac{w\,t}{d^2}}{\ln \frac{w\,t}{d^2}}. \tag{27}$$

(26) and (27) is just a short notation for the following statement: There exists a possibly large but universal constant $C < \infty$ such that whenever

$$\frac{d^2}{t} \;\leq\; \frac{1}{C}\, w,$$

we have

$$\frac{1}{C}\,\frac{\ln\ln \frac{w\,t}{d^2}}{\ln \frac{w\,t}{d^2}} \;\leq\; \frac{\ln \frac{w\,t}{d^2}}{t^2}\, e_{thin}(d,t,w) \;-\; \pi \;\leq\; C\,\frac{\ln\ln \frac{w\,t}{d^2}}{\ln \frac{w\,t}{d^2}}.$$

In case of a Néel wall limited by anisotropy, a similar scaling law, with a less explicit correction term, has been announced in [2, Theorem 3.2]. The proof of this related scaling law without the correction term can be found in [4, Chapter 3.4.2]. Our proof of Proposition 2 essentially follows the same strategy. A finer analysis of the minimizer itself, which in particular captures its logarithmic tail, is in [8], again in the case of a Néel wall limited by anisotropy. This requires a rather subtle analysis which is quite different from ours.

Let us briefly address the following three questions

A) Could we have guessed the scaling (27)?

B) When does the thin–film approximation seem reasonable?

C) Which predictions w. r. t. μ may be drawn from Proposition 2?

Question A): Observe that in the thin–film approximation (25), the magnetostatic energy is the square of the homogeneous $H^{\frac{1}{2}}((-w,w))$–norm of m_1

$$\sum_{n_1} \frac{\pi\,|n_1|}{2\,w}\,|m_{1,n_1}|^2 \;=\; \frac{1}{2}\,\|(\frac{d}{dx_1})^{\frac{1}{2}} m_1\|^2_{L^2((-w,w))}.$$

Hence, as opposed to (20), (25) keeps the nonlocal character of (12). Without the exchange–energy term, the infimum e_{thin} would be zero, since $H^{\frac{1}{2}}((-w,w))$ fails to embed into $L^\infty((-w,w))$: One can construct a sequence of winding magnetizations (13) with vanishing $H^{\frac{1}{2}}((-w,w))$–norm. Hence we expect

$$e_{thin}(d,t,w) \;\ll\; t^2 \quad \text{for} \quad \frac{w\,t}{d^2} \;\gg\; 1,$$

the latter being the single non–dimensional parameter. The failure of the embedding of $H^{\frac{1}{2}}((-w,w))$ into $L^\infty((-w,w))$ is a consequence of the failure of the embedding of H^1 into L^∞ in two space dimensions (since $H^{\frac{1}{2}}((-w,w))$ is the space of traces of $H^1((-w,w)\times I\!R)$–functions), which is a classical fact: H^1–functions may have a logarithmic singularity. But this embedding barely fails: The spaces $H^{\frac{1}{2}}((-w,w))$ and $L^\infty((-w,w))$ have the same scaling — both are scale invariant in fact. Hence it is not surprising that a logarithm appears in Proposition 2

$$e_{thin}(d,t,w) \;\sim\; t^2\,\ln^{-1}\frac{w\,t}{d^2} \quad \text{for} \quad \frac{w\,t}{d^2} \;\gg\; 1.$$

The fact that the correction term contains a double logarithm is not so obvious — it is a consequence of the nonlinearity — and requires some work.

Question B): The proof of Proposition 2 suggests that the minimizer has a core and a logarithmic tail with

$$\begin{aligned} \text{size of core} &\sim \frac{d^2}{t} \quad \text{possibly modulo a logarithm,} \\ \text{size of logarithmic tail} &\sim w, \end{aligned}$$

This gives an additional meaning to the condition (26). In particular, the smallest length scale is of order $\frac{d^2}{t}$. This scale is much larger than the film thickness t if and only if

$$t \ll d. \tag{28}$$

Hence we expect (27) to be a good approximation as long as (28) is satisfied. In Subsection 4.3, we shall see that this is too pessimistic by a logarithm.

Question C): In view of the answer to B), Proposition 2 predicts that for sufficiently thin films in the sense of (28) and for sufficiently far–away walls in the sense of (26), we have

$$\frac{1}{d}\,\mu(d,t,w) \;\approx\; \frac{1}{d}\,\mu_{thin}(d,t,w) \;\approx\; -\pi\,\left(\frac{t}{d}\right)^2\,\frac{d}{w}\,\ln^{-2}\frac{w\,t}{d^2}. \tag{29}$$

We obtain a quadratic growth of the potential in t instead of the desired sublinear growth (19). Also the correction term does not indicate a cross–over in the t–scaling to sublinear growth.

4.3 The intermediate regime

So far, we were not successful in identifying a regime with (19), c.f. (24) and (29). We studied both extreme regimes and thereby necessarily covered the two possible leading order scalings of e. But of course we did not cover all possible first order corrections that way — there will be more than the two extreme regimes for the first order correction, which we call intermediate regimes. Since w does not appear at leading order in the thick–film regime, it is indeed important to look at the first order corrections. In some intermediate regime, the first order correction will be determined by the cross–over in f. This is our only chance to uncover a regime with (19). More precisely, the only chance is an intermediate regime, where the leading order scaling is à la thick–film (and thus w–independent) but where the first order correction comes from the cross–over in f. This is exactly what we will do in Theorem 1.

From experiments, it is well–known that these intermediate regimes (which must be close to $t \sim d$) are very rich: It is at these thicknesses where one observes the transition from Néel to cross–tie wall and from cross–tie wall to the asymmetric Bloch wall [7, Fig.3.79].

Theorem 1 *Suppose the wall distance is sufficiently large and the film is moderately thick in the sense of*

$$d \ll w \quad \textit{and} \quad \ln \frac{w}{d} \ll \frac{t}{d} \ll \frac{w}{d}. \tag{30}$$

Then we have

$$\frac{1}{d\,t}\, e(d,t,w) - 8 \approx -4\,\pi\,\frac{d}{t}\,\ln\frac{w}{d}.$$

An ad–hoc analytic approximation of the minimizer in an analogous regime was given in [10]. As noted earlier, only the case of walls limited by anisotropy is considered in [10].

Let us address two questions

A) What predictions w. r. t. μ may be drawn from Theorem 1?

B) To what extent could we have guessed Theorem 1 from Propositions 1 and 2?

Question A): We indeed have identified a regime, namely (30) in which we have

$$\frac{1}{d}\,\mu(d,t,w) \approx -4\,\pi\,\frac{d}{w} \quad !$$

Question B): As can be easily checked, the cross–over between the leading order of e_{thick} in (22) and e_{thin} in (27) happens for moderate thicknesses

$$\frac{t}{d} \sim \ln\frac{w}{d}.$$

Hence we would indeed have guessed the leading order

$$e(d,t,w) \approx \left\{ \begin{array}{cc} 8\,d\,t & \text{for } \frac{t}{d} \gg \ln\frac{w}{d} \\ \pi\,t^2\,\ln^{-1}\frac{w\,t}{d^2} & \text{for } \frac{t}{d} \ll \ln\frac{w}{d} \end{array} \right\}.$$

We also can successfully guess the scaling of the correction term: We start by observing that the Fourier multiplier is dominated by either homogeneous approximation

$$f(z) \le \min\{z, 1\}.$$

This implies of course that

$$E(m') \le \min\{E_{thick}(m'), E_{thin}(m')\}$$

and therefore

$$e(d,t,w) \le \min\{e_{thick}(d,t,w), e_{thin}(d,t,w)\}. \tag{31}$$

Moreover, as we pointed out in Subsections 4.1 and 4.2, the minimizer of E_{thick},

$$m^*_{thick} \text{ lives on length scales } d, \tag{32}$$

whereas the minimizer of E_{thin},

$$m^*_{thin} \text{ lives on length scales from } \frac{d^2}{t} \text{ to } w. \tag{33}$$

Therefore it seems reasonable that the true Néel wall m^* combines features of the thick–film Néel wall and the thin–film Néel wall. A certain fraction of the rotation of m' near the center is done according to the narrow thick–film scenario, the remainder is done in line with the broad thin–film scenario. To fix ideas, let us think of a convex combination on the level of the m_1–component

$$m^*_1 \;=\; \lambda\, m^*_{1,thick} + (1-\lambda)\, m^*_{1,thin},$$

which ensures $m^*_1(0) = 1$. Since the magnetostatic energy is quadratic in m_1 (and the exchange energy at least strictly convex in m_1, see Lemma 8 below), and thanks to the separation of scales (32) & (33), it seems reasonable to assume that

$$\begin{aligned} E(m^*) &\approx \lambda^2\, E(m^*_{thick}) + (1-\lambda)^2\, E(m^*_{thin}) \\ &\approx \lambda^2\, E_{thick}(m^*_{thick}) + (1-\lambda)^2\, E_{thin}(m^*_{thin}). \end{aligned}$$

Optimizing in λ would yield

$$\frac{1}{e} \;\approx\; \frac{1}{e_{thick}} + \frac{1}{e_{thin}}$$

— a refinement of (31). We now plug in the leading order expressions from Propositions 1 and 2

$$\begin{aligned} \frac{1}{e} &\approx \frac{1}{8\,d\,t} + \frac{\ln \frac{w\,t}{d^2}}{\pi\, t^2} \\ &= \frac{1}{8\,d\,t}\left(1 + (\ln \frac{w\,t}{d^2})\,\frac{8}{\pi}\,\frac{d}{t}\right). \end{aligned} \tag{34}$$

We observe that (30) implies $1 \ll \ln \frac{t}{d} \ll \ln \frac{w}{d}$, so that

$$\ln \frac{w\,t}{d^2} \;=\; \ln \frac{w}{d} + \ln \frac{t}{d} \;\approx\; \ln \frac{w}{d}. \tag{35}$$

Therefore, again according to (30), $(\ln \frac{w\,t}{d^2})\,\frac{d}{t}$ is a small perturbation in (34). Hence we would obtain

$$\frac{1}{d\,t}\,e - 8 \;\approx\; -(\ln \frac{w\,t}{d^2})\,\frac{64}{\pi}\,\frac{d}{t} \;\overset{(35)}{\approx}\; -\frac{64}{\pi}\,\frac{d}{t}\,\ln \frac{w}{d},$$

which gives the right scaling for the correction term, but the wrong constant. It is not surprising that the constant is wrong since the functional is not quadratic in m_1, which matters for the thick–film wall.

5 Proofs

5.1 Proof of Proposition 1

It is convenient to measure length and energy in the reduced units

$$x_1 \;=\; d\,\hat{x}_1 \quad \text{and} \quad E_{thin} \;=\; d\,t\,\hat{E}_{thick}.$$

Then

$$\begin{aligned}\hat{E}_{thick}(m') \;&=\; \int_{-\hat{w}}^{\hat{w}} |\frac{dm'}{d\hat{x}_1}|^2\, d\hat{x}_1 + \int_{-\hat{w}}^{\hat{w}} m_1^2\, d\hat{x}_1 \\ &=\; \int_{-\hat{w}}^{\hat{w}} (\frac{d\theta}{d\hat{x}_1})^2\, d\hat{x}_1 + \int_{-\hat{w}}^{\hat{w}} \cos^2\theta\, d\hat{x}_1 \;=\; \hat{E}_{thick}(\theta),\end{aligned}$$

where there is a single non–dimensional parameter $\hat{w}$

$$\hat{w} \;:=\; \frac{w}{d} \;\overset{(21)}{\gg}\; 1. \tag{36}$$

Our goal is to show that in the regime (36),

$$\min_{\theta} \hat{E}_{thick}(\theta) - 8 \;\approx\; 2\,\exp(-\hat{w}), \tag{37}$$

where the minimum is taken over all θ with

$$\theta(\hat{x}_1 + \hat{w}) \;=\; \theta(\hat{x}_1) + \pi. \tag{38}$$

In the sequel, we will drop the hats.

This variational problem admits a minimizer θ^*. The Euler–Lagrange equation is given by

$$-2\,\frac{d^2\theta^*}{dx^2} + \frac{d}{d\theta^*}(\cos^2\theta^*) \;=\; 0.$$

The first integral is

$$\frac{d}{dx}\,[-(\frac{d\theta^*}{dx})^2 + \cos^2\theta^*] \;=\; 0.$$

According to (38), the range of θ^* is $\mathbb{R}$. Therefore $\cos^2\theta^*$ will be zero for some x. Hence there exists an $\epsilon \geq 0$ s. t.

$$(\frac{d\theta^*}{dx})^2 \;=\; \cos^2\theta^* + \epsilon^2.$$

The case $\epsilon \;=\; 0$ is ruled out as a solution of $(\frac{d\theta^*}{dx})^2 = \cos^2\theta^*$ could never satisfy (38). Hence $\epsilon > 0$. Since θ^* is smooth and cannot — in view of (38) — be monotone decreasing, we must have

$$\frac{d\theta^*}{dx} \;=\; (\cos^2\theta^* + \epsilon^2)^{\frac{1}{2}}. \tag{39}$$

Thanks to a translation, we may always assume

$$\theta^*(0) \;=\; 0 \;\stackrel{(38)}{\Longrightarrow}\; \theta^*(\pm w) \;=\; \pm\pi. \tag{40}$$

It then follows from (39) that

$$\theta^* \text{ is a monotone map from } (-w, w) \text{ onto } (-\pi, \pi). \tag{41}$$

ϵ is implicitly determined by

$$\int_0^{\pi} \frac{1}{(\cos^2\theta + \epsilon^2)^{\frac{1}{2}}}\, d\theta \;\stackrel{(41)}{=}\; \int_0^{w} \frac{1}{(\cos^2\theta^* + \epsilon^2)^{\frac{1}{2}}} \frac{d\theta^*}{dx_1}\, dx_1 \;\stackrel{(39)}{=}\; w$$

or – by symmetry –

$$\int_0^{\frac{\pi}{2}} \frac{1}{(\cos^2\theta + \epsilon^2)^{\frac{1}{2}}}\, d\theta \;=\; \frac{w}{2}. \tag{42}$$

Since the l. h. s. of (42), i. e.

$$\int_0^{\frac{\pi}{2}} \frac{1}{(\cos^2\theta + \epsilon^2)^{\frac{1}{2}}}\, d\theta \tag{43}$$

is bounded if ϵ is bounded away from zero, we deduce from (36) that necessarily

$$\epsilon \;\ll\; 1. \tag{44}$$

On the other hand (43) diverges logarithmically for $\epsilon = 0$ due to the singularity at $\theta = \frac{\pi}{2}$. Hence

$$\int_0^{\frac{\pi}{2}} \frac{1}{(\cos^2\theta + \epsilon^2)^{\frac{1}{2}}}\, d\theta \;\stackrel{(44)}{\approx}\; \int_0^{\frac{\pi}{2}} \frac{1}{((\theta - \frac{\pi}{2})^2 + \epsilon^2)^{\frac{1}{2}}}\, d\theta \;\stackrel{(44)}{\approx}\; \ln\frac{1}{\epsilon}$$

and thus by (42)

$$\epsilon \;\approx\; \exp(-\frac{w}{2}). \tag{45}$$

We now have all the ingredients to analyze the minimal energy

$$\begin{aligned}
e(\epsilon) \quad &:= \quad \int_{-w}^{w} (\frac{d\theta^*}{dx_1})^2\, dx_1 + \int_{-w}^{w} \cos^2\theta^*\, dx_1 \\
&\stackrel{(39),(41)}{=} \quad \int_{-\pi}^{\pi} (\cos^2\theta + \epsilon^2)^{\frac{1}{2}}\, d\theta + \int_{-\pi}^{\pi} \frac{\cos^2\theta}{(\cos^2\theta + \epsilon^2)^{\frac{1}{2}}}\, d\theta \\
&= \quad \int_{-\pi}^{\pi} \frac{2\,\cos^2\theta + \epsilon^2}{(\cos^2\theta + \epsilon^2)^{\frac{1}{2}}}\, d\theta \\
&= \quad 4 \int_0^{\frac{\pi}{2}} \frac{2\,\cos^2\theta + \epsilon^2}{(\cos^2\theta + \epsilon^2)^{\frac{1}{2}}}\, d\theta.
\end{aligned}$$

We observe

$$e(0) \;=\; 8 \int_0^{\frac{\pi}{2}} \cos\theta\, d\theta \;=\; 8. \tag{46}$$

and

$$\frac{de}{d\epsilon} \;=\; 4\,\epsilon^3 \int_0^{\frac{\pi}{2}} \left(\frac{1}{\cos^2\theta + \epsilon^2}\right)^{\frac{3}{2}}\, d\theta.$$

Since the last integral diverges for $\epsilon = 0$ due to the singularity at $\theta = \frac{\pi}{2}$, we have according to (44)

$$\begin{aligned}
\frac{de}{d\epsilon} \;&\approx\; 4 \int_0^{\frac{\pi}{2}} \left(\frac{\epsilon^2}{(\theta - \frac{\pi}{2})^2 + \epsilon^2}\right)^{\frac{3}{2}}\, d\theta \\
&=\; 4\,\epsilon \int_0^{\frac{\pi}{2\,\epsilon}} \left(\frac{1}{\hat\theta^2 + 1}\right)^{\frac{3}{2}}\, d\hat\theta \\
&\approx\; 4\,\epsilon \int_0^{\infty} \left(\frac{1}{\hat\theta^2 + 1}\right)^{\frac{3}{2}}\, d\hat\theta \;=\; 4\,\epsilon \int_0^{\infty} \frac{d}{d\hat\theta}\left(\frac{\hat\theta}{\sqrt{\hat\theta^2 + 1}}\right) d\hat\theta \;=\; 4\,\epsilon. \qquad (47)
\end{aligned}$$

From (46) and (47) we obtain as desired

$$e(\epsilon) - 8 \;\approx\; 2\,\epsilon^2 \;\overset{(45)}{\approx}\; 2\,\exp(-w).$$

□

5.2 Proof of Proposition 2

It is convenient to measure length and energy in the reduced units

$$x_1 \;=\; w\,\hat x_1 \quad \text{and} \quad E_{thin} \;=\; t^2\,\hat E_{thin}.$$

Then

$$\hat E_{thin}(m') \;=\; \epsilon \int_{-1}^{1} |\frac{dm'}{d\hat x_1}|^2\, d\hat x_1 \;+\; \sum_{\hat n_1} \frac{\pi\,|\hat n_1|}{2}\,|m_{1,\hat n_1}|^2, \qquad (48)$$

where

$$m_{1,\hat n_1} \;=\; \frac{1}{\sqrt{2}} \int_{-1}^{1} e^{i\,\pi\,\hat n_1\,\hat x_1}\, m_1(\hat x_1)\, d\hat x_1$$

and ϵ is the single nondimensional parameter

$$\epsilon \;:=\; \frac{d^2}{t\,w} \;\overset{(26)}{\ll}\; 1.$$

Our goal is to show that in this regime,

$$(\ln\frac{1}{\epsilon})\, \min_{m'} \hat E_{thin}(m') - \pi \;\sim\; \frac{\ln\ln\frac{1}{\epsilon}}{\ln\frac{1}{\epsilon}}, \qquad (49)$$

where the min is taken over all m' of the form (10) with

$$\theta(\hat x_1 + 1) \;=\; \theta(\hat x_1) + \pi. \qquad (50)$$

In the sequel, we will drop the hats. The upper bound with the scaling indicated in (49) will be established in Lemma 4, the lower bound in Lemma 7.

We start with a few observations. Because of $|m'|^2 = 1$, E_{thin} can be expressed in terms of $m_1 \in [-1,1]$ alone:

$$E_{thin}(m_1) \;=\; \epsilon \int_{-1}^{1} \frac{1}{1-m_1^2} (\frac{dm_1}{dx_1})^2 \, dx_1 \;+\; \sum_{\hat{n}_1} \frac{\pi \, |n_1|}{2} \, |m_{1,n_1}|^2$$

with the understanding that

$$\frac{1}{1-m_1^2} (\frac{dm_1}{dx_1})^2 \;=\; \left\{ \begin{array}{cc} +\infty & \text{if } m_1 = \pm 1 \text{ and } \frac{dm_1}{dx_1} \neq 0 \\ 0 & \text{if } m_1 = \pm 1 \text{ and } \frac{dm_1}{dx_1} = 0 \end{array} \right\}.$$

Furthermore, (50) implies that there exists an x_0 with $m_1(x_0) = 1$, so that by translation invariance of the integrand we may assume w.l.o.g.

$$m_1(0) \;=\; 1.$$

Hence we have to minimize E_{thin} among all $m_1 : I\!R \to [-1,1]$ with

$$m_1(x_1+1) \;\stackrel{(50)}{=}\; -m_1(x_1) \quad \text{and} \quad m_1(0) \;=\; 1. \tag{51}$$

In a first pass, we will replace E_{thin} by the quadratic functional $\tilde{E}_{thin}$

$$E_{thin}(m_1) \;\geq\; \epsilon \int_{-1}^{1} (\frac{dm_1}{dx_1})^2 \, dx_1 \;+\; \sum_{n_1} \frac{\pi \, |n_1|}{2} \, |m_{1,n_1}|^2 \;=:\; \tilde{E}_{thin}(m_1). \tag{52}$$

Let m_1^* denote the minimizer of $\tilde{E}_{thin}$ among all m_1 with (51). The first lemma gives the explicit formula for m_1^* in Fourier space.

Lemma 1 *The Fourier coefficients of m_1^* are given by*

$$m_{1,n_1}^* \;=\; \frac{1}{\lambda^*} \left\{ \begin{array}{cc} \frac{\sqrt{2}}{2\,\pi\,\epsilon\,n_1^2 + |n_1|} & \textit{for } n_1 \textit{ odd} \\ 0 & \textit{for } n_1 \textit{ even} \end{array} \right\}, \tag{53}$$

where

$$|\lambda^* - \ln \frac{1}{\epsilon}| \;\lesssim\; 1. \tag{54}$$

We also have

$$|(\ln \frac{1}{\epsilon}) \, \tilde{E}_{thin}(m_1^*) - \pi| \;\lesssim\; \ln^{-1} \frac{1}{\epsilon}. \tag{55}$$

In view of (52), this yields the suboptimal lower bound

$$(\ln \frac{1}{\epsilon}) \, \min_{m'} E_{thin} - \pi \;\gtrsim\; \frac{1}{\ln \frac{1}{\epsilon}}, \tag{56}$$

which we will improve upon towards the end of the proof of Proposition 2. But first we consider the upper bound. We cannot use m_1^* as an upper–bound construction — its energy is infinite

$$E_{thin}(m_1^*) \;=\; +\infty.$$

Indeed, the variational problem for m_1^* is a compact perturbation of

$$\text{minimze} \quad \epsilon \int_{-1}^{1} (\frac{dm_1}{dx_1})^2 \, dx_1 \quad \text{among all } m_1 \text{ with (51).}$$

Hence we expect

$$-\frac{dm_1^*}{dx_1}(0+) \;=\; \frac{dm_1^*}{dx_1}(0-) \;>\; 0.$$

We thus need another approach for the upper–bound construction: Lemma 1 suggests to view m_1^* as a regularized (on length scale ϵ) and normalized (by λ^*) version of the function ϕ_0 given by its Fourier coefficients $\phi_{0,n_1} = \frac{\sqrt{2}}{|n_1|}$ for n_1 odd and $\phi_{0,n_1} = 0$ for n_1 even. For the upper–bound construction, we will consider a different regularization ϕ_δ (on lengthscale δ) of ϕ: the harmonic extension of ϕ_0. Lemma 2 identifies the real–space representation of ϕ_δ.

Lemma 2 *The function*

$$\phi_\delta(x_1) \;:=\; \sum_{n_1} (-1)^{n_1} \, \ln \frac{1}{\sqrt{(x_1 - n_1)^2 + \delta^2}} \tag{57}$$

is well defined and has the Fourier coefficients

$$\phi_{\delta,n_1} \;=\; \left\{ \begin{array}{cc} \frac{\sqrt{2}}{|n_1|} \exp(-\pi \, |n_1| \, \delta) & \textit{for } n_1 \textit{ odd} \\ 0 & \textit{for } n_1 \textit{ even} \end{array} \right\}. \tag{58}$$

In Lemma 3, we will estimate the energy of the normalized ϕ_δ. We then optimize in δ ($\delta = \epsilon \, \ln \frac{1}{\epsilon}$) and so obtain the desired upper bound.

Lemma 3 *We have*

$$(\ln \frac{1}{\epsilon}) \, \min_{m'} E_{thin}(m') - \pi \;\lesssim\; \frac{\ln \ln \frac{1}{\epsilon}}{\ln \frac{1}{\epsilon}}. \tag{59}$$

The remainder of the proof is devoted to filling the gap between (56) and (59). Obviously, we may not totally neglect the nonlinearity in the exchange energy, as done for (56). The idea is to interpret E_{thin} as a perturbation of $\tilde{E}_{thin}$:

$$E_{thin}(m_1) \;=\; \tilde{E}_{thin}(m_1) + \epsilon \int_{-1}^{1} \frac{m_1^2}{1 - m_1^2} (\frac{dm_1}{dx_1})^2 \, dx_1$$

and to write the minimizer m_1 of E_{thin} with (51) as a perturbation of the minimizer m_1^* of $\tilde{E}_{thin}$

$$\zeta_1 \;=\; m_1 - m_1^* \quad \text{satisfies} \quad \zeta_1(x_1+1) \;=\; -\zeta_1(x_1) \quad \text{and} \quad \zeta_1(0) = 0. \tag{60}$$

Since $\tilde{E}_{thin}$ is a quadratic functional and m_1^* its minimizer, we have

$$\tilde{E}_{thin}(m_1) - \tilde{E}_{thin}(m_1^*) \;=\; \tilde{E}_{thin}(\zeta_1).$$

Hence we may write

$$E_{thin}(m_1) \;=\; \tilde{E}_{thin}(m_1^*) + \tilde{E}_{thin}(\zeta_1) + \epsilon \int_{-1}^{1} \frac{m_1^2}{1-m_1^2} (\frac{dm_1}{dx_1})^2 \, dx_1, \tag{61}$$

which is our starting point.

We first show that m_1^* has indeed a logarithmic tail outside a core region of size ϵ.

Lemma 4 *We have*

$$|\lambda^* \, m_1^* - \phi_0| \;\lesssim\; \left(\frac{\epsilon}{|x_1|}\right)^2 \quad \textit{for} \quad 0 < |x_1| \ll 1.$$

We now bound the last term in (61), i. e. the nonlinear perturbation, from below by a linear term which is much larger than the linearized exchange energy, at least in the core region.

Lemma 5 *For*

$$\delta \;:=\; \epsilon \, \frac{\ln^{\frac{2}{3}} \frac{1}{\epsilon}}{(\ln\ln \frac{1}{\epsilon})^{\frac{1}{3}}} \;\gg\; \epsilon, \tag{62}$$

we have

$$\epsilon \int_{-1}^{1} \frac{m_1^2}{1-m_1^2} (\frac{dm_1}{dx_1})^2 \, dx_1 \;\gtrsim\; \delta \int_{\epsilon}^{\delta} (\frac{dm_1}{dx_1})^2 \, dx_1. \tag{63}$$

The next lemma is crucial in getting the correct order of the correction term, i. e. $\frac{\ln\ln\frac{1}{\epsilon}}{\ln\frac{1}{\epsilon}}$ in the lower bound.

Lemma 6 *Let*

$$\epsilon \;\ll\; \delta \;\ll\; 1. \tag{64}$$

Let the 2–periodic function u have a logarithmic behavior over (ϵ, δ) in the sense of

$$\int_{\alpha}^{2\,\alpha} (u - \bar{u})^2 \, dx_1 \;\gtrsim\; \alpha \quad \textit{for all } \epsilon \ll \alpha \ll \delta, \tag{65}$$

where $\bar{u}$ denotes the mean value of u on $(\alpha, 2\,\alpha)$. Then we have for any 2–periodic function ζ

$$\sum_{n_1} \frac{\pi \, |n_1|}{2} \, |\zeta_{n_1}|^2 + \delta \int_{\epsilon}^{\delta} (\frac{d}{dx_1}(\zeta - u))^2 \, dx_1 \;\gtrsim\; \ln\frac{\delta}{\epsilon}.$$

Together with (55), the last lemma establishes the desired lower bound:

Lemma 7 *We have*

$$(\ln \frac{1}{\epsilon}) \, \Big(E_{thin}(m_1) - \tilde{E}_{thin}(m_1^*) \Big) \; \gtrsim \; \frac{\ln \ln \frac{1}{\epsilon}}{\ln \frac{1}{\epsilon}}.$$

PROOF OF LEMMA 1. $\tilde{E}_{thin}$ has a nice representation in terms of its Fourier coefficients

$$\tilde{E}_{thin}(m_1) \; = \; \frac{\pi}{2} \, \sum_{n_1} \Big(2 \, \pi \, \epsilon \, n_1^2 + |n_1| \Big) \; |m_{1,n_1}|^2.$$

On the level of the Fourier coefficients, (51) translates into

$$\bar{m}_{1,n_1} \; = \; m_{1,-n_1}, \quad m_{1,n_1} \; = \; 0 \;\; \text{for } n_1 \text{ even}, \quad \text{and} \quad \sum_{n_1} m_{1,n_1} \; = \; \sqrt{2}, \tag{66}$$

where the bar denotes complex conjugation. The minimization of $\tilde{E}_{thin}$ among all $\{m_{1,n_1}\}_{n_1}$ with (66) can be carried out explicitly. The Fourier coefficients of the minimizer m_1^* are indeed given by (53), where Lagrange multiplier λ^* ensures the last condition in (66), and hence has to be chosen as

$$\lambda^* \; := \; \sum_{n_1 \; odd} \frac{1}{2 \, \pi \, \epsilon \, n_1^2 + |n_1|}.$$

In particular, we have

$$\tilde{E}(m_1^*) \; = \; \frac{\pi}{\lambda^*}. \tag{67}$$

Let us now show (54). Indeed, on one hand we have

$$\begin{aligned} \int_1^\infty \frac{1}{2 \, \pi \, \epsilon \, z^2 + z} \, dz \; &= \; \int_1^\infty \frac{d}{dz} \Big(\ln \frac{z}{2 \, \pi \, \epsilon \, z + 1} \Big) \, dz \\ &= \; \ln \frac{1 + 2 \, \pi \, \epsilon}{2 \, \pi \, \epsilon} \; = \; \ln \frac{1}{\epsilon} - \ln \frac{2 \, \pi}{1 + 2 \, \pi \, \epsilon}, \end{aligned}$$

so that

$$\int_1^\infty \frac{1}{2 \, \pi \, \epsilon \, z^2 + z} \, dz - \ln \frac{1}{\epsilon} \; \approx \; - \ln \, 2 \, \pi \; \sim \; -1.$$

On the other hand,

$$\begin{aligned} &\sum_{n_1 \; odd} \frac{1}{2 \, \pi \, \epsilon \, n_1^2 + |n_1|} - \int_1^\infty \frac{1}{2 \, \pi \, \epsilon \, z^2 + z} \, dz \\ &\quad = \; \sum_{\substack{n_1 \; odd \\ n_1 \geq 1}} \int_{n_1}^{n_1 + 2} \left(\frac{1}{2 \, \pi \, \epsilon \, n_1^2 + n_1} - \frac{1}{2 \, \pi \, \epsilon \, z^2 + z} \right) dz \\ &\quad \approx \; \sum_{\substack{n_1 \; odd \\ n_1 \geq 1}} \int_{n_1}^{n_1 + 2} \left(\frac{1}{n_1} - \frac{1}{z} \right) dz \; \sim \; \sum_{\substack{n_1 \; odd \\ n_1 \geq 1}} \frac{1}{n_1^2} \; \sim \; 1. \end{aligned}$$

This proves (54).

In view of (67), (54) implies (55):

$$|(\ln\frac{1}{\epsilon})\,\tilde{E}(m_1^*)-\pi| \overset{(67)}{=} \frac{\pi}{\lambda^*}\,|\ln\frac{1}{\epsilon}-\lambda^*| \overset{(54)}{\lesssim} \frac{1}{\lambda^*} \overset{(54)}{\approx} \ln^{-1}\frac{1}{\epsilon}.$$

□

Proof of Lemma 2.

We start by arguing that (57) is well–defined. In fact, ϕ_δ is the harmonic extension $\bar{\phi}$ of ϕ_0 in the two variables (x_1,x_3), evaluated at $x_3=\delta$. We will argue that the latter, i. e.

$$\bar{\phi}(x_1,x_3) \;=\; \sum_{n_1}(-1)^{n_1}\,\ln\frac{1}{((x_1-n_1)^2+x_3^2)^{\frac{1}{2}}} \tag{68}$$

is well–defined. Indeed, since we can write $\bar{\phi}$ as

$$\bar{\phi}(x_1,x_3) \;=\; \sum_{n_1\,even}\tilde{\phi}(x_1+n_1,x_3), \tag{69}$$

where the second order difference

$$\tilde{\phi}(x_1,x_3) \;:=\; \ln\frac{1}{(x_1^2+x_3^2)^{\frac{1}{2}}}-\frac{1}{2}\,\ln\frac{1}{((x_1-1)^2+x_3^2)^{\frac{1}{2}}}-\frac{1}{2}\,\ln\frac{1}{((x_1+1)^2+x_3^2)^{\frac{1}{2}}}$$

has good decay properties, i. e.

$$|\tilde{\phi}(x_1,x_3)| \;\lesssim\; \frac{1}{x_1^2+x_3^2} \quad \text{for } x_1^2+x_3^2 \;\gg\; 1,$$

$\bar{\phi}$ is well–defined.

We now give the argument in favor of (58). The function (68) of two variables is known to be a fundamental solution:

$$-\left(\frac{\partial^2\bar{\phi}}{\partial x_1^2}+\frac{\partial^2\bar{\phi}}{\partial x_3^2}\right) \;=\; 2\,\pi\sum_{n_1}(-1)^{n_1}\,\delta((x_1,x_3)-(n_1,0)).$$

In particular, it indeed has the symmetries as suggested by the formal representation (57), that is,

$$\bar{\phi}(x_1+1,x_3) \;=\; -\bar{\phi}(x_1,x_3).$$

Hence if the function $\rho\colon I\!R\to I\!R$ has the same symmetry as $\phi_0(x_1)$, that is,

$$\rho(x_1+1) \;=\; -\rho(x_1), \tag{70}$$

the convolution

$$u(x_1,x_3) \;:=\; \int_{-1}^{1}\bar{\phi}(x_1-y_1,x_3)\,\rho(y_1)\,dy_1 \tag{71}$$

solves

$$\begin{aligned} -\left(\frac{\partial^2 u}{\partial x_1^2}+\frac{\partial^2 u}{\partial x_3^2}\right)(x_1,x_3) &= 0 \quad \text{for } x_3 \neq 0, \\ -\left(\frac{\partial u}{\partial x_3}(x_1,0+)-\frac{\partial u}{\partial x_3}(x_1,0-)\right) &= 4\,\pi\,\rho(x_1). \end{aligned}$$

From this, we gather that

$$u(x_1,x_3) \;=\; \sum_{n_1} u_{n_1}\,\exp(-\pi\,|n_1||x_3|)\,\frac{1}{\sqrt{2}}\,e^{i\,\pi\,n_1\,x_1}, \tag{72}$$

where the Fourier coefficients u_{n_1} of $u(x_1,x_3=0)$ are related to those of ρ by

$$u_{n_1} \;=\; \frac{2}{|n_1|}\,\rho_{n_1}. \tag{73}$$

On the other hand, we deduce from (71)

$$u_{n_1} \;=\; \sqrt{2}\,\phi_{0,n_1}\,\rho_{n_1}. \tag{74}$$

Since the real functions ϕ_0 and ρ obey the same symmetry (70), we infer (58) for $\delta=0$ from (73) and (74). Like in (72), we have

$$\phi_{\delta,n_1} \;=\; \exp(-\pi\,|n_1|\,\delta)\,\phi_{0,n_1}.$$

This yields (58) for $\delta>0$. □

Proof of Lemma 3.
Our Ansatz for the upper bound construction m_1 is the normalized ϕ_δ from Lemma 2, i. e.

$$m_1(x_1) \;:=\; \frac{\phi_\delta(x_1)}{\phi_\delta(0)}, \tag{75}$$

where the length scale $\delta \ll 1$ will be chosen at the end of the proof of this lemma. One can see from a resummation as in (69) that ϕ_δ attains its maximum in $x_1 \in \{\cdots,-2,0,2,\cdots\}$. Hence $|\phi_\delta|$ attains its maximum for $x_1 \in \mathbb{Z}$. Therefore (75) defines an m_1 with $|m_1|\le 1$ and $|m_1|=1$ if and only if $x_1\in\mathbb{Z}$. We will show that exchange and magnetostatic energy behave as

$$\epsilon\int_{-1}^{1}\frac{1}{1-m_1^2}\,(\frac{dm_1}{dx_1})^2\,dx_1 \;\lesssim\; \frac{\epsilon}{\delta}\,\ln^{-1}\frac{1}{\delta}, \tag{76}$$

$$\sum_{n_1}|n_1|\,|m_{1,n_1}|^2 - 2\,\ln^{-1}\frac{1}{\delta} \;\lesssim\; \ln^{-2}\frac{1}{\delta}. \tag{77}$$

At the end of the proof, we will select δ.

Let us begin with the estimate of the linear magnetostatic energy (77) for which we use the Fourier representation of ϕ_δ. In view of

$$|\phi_\delta(0) - \ln\frac{1}{\delta}| \;\lesssim\; 1, \tag{78}$$

(77) amounts to

$$\sum_{n_1} |n_1||\phi_{\delta,n_1}|^2 - 2\,\ln\frac{1}{\delta} \;\lesssim\; 1; \tag{79}$$

indeed:

$$\begin{aligned}
&\sum_{n_1} |n_1||m_{1,n_1}|^2 - 2\,\ln^{-1}\frac{1}{\delta} \\
&\quad= \frac{1}{\phi_\delta(0)^2}\left(\sum_{n_1} |n_1||\phi_{\delta,n_1}|^2 - 2\,\ln\frac{1}{\delta}\right) + \frac{2\,(\ln\frac{1}{\delta}+\phi_\delta(0))}{\phi_\delta(0)^2\,\ln\frac{1}{\delta}}\,(\ln\frac{1}{\delta}-\phi_\delta(0)) \\
&\quad\overset{(79)}{\lesssim} \frac{1}{\phi_\delta(0)^2} + \frac{2\,(\ln\frac{1}{\delta}+\phi_\delta(0))}{\phi_\delta(0)^2\,\ln\frac{1}{\delta}}\,(\ln\frac{1}{\delta}-\phi_\delta(0)) \\
&\quad\overset{(78)}{\lesssim} \ln^{-2}\frac{1}{\delta}.
\end{aligned}$$

We now argue in favor of (79). According to Lemma 2, we have

$$\sum_{n_1} |n_1||\phi_{\delta,n_1}|^2 \;=\; 2\sum_{n_1\,odd}\frac{1}{|n_1|}\,\exp(-2\,\pi\,|n_1|\,\delta).$$

Therefore (79) can be proved using the same argument we used for (54).

Let us now consider the nonlinear exchange energy (76) for which we use the real–space representation of ϕ_δ. We will argue that the leading order contribution to the exchange energy on $(-\frac{1}{2},\frac{1}{2})$ comes from the "near–field"

$$\begin{aligned}
\tilde\phi_\delta(x_1) &:= \ln\frac{1}{(x_1^2+\delta^2)^{\frac{1}{2}}}, \\
\tilde m_1(x_1) &:= \frac{\tilde\phi_\delta(x_1)}{\tilde\phi_\delta(0)}.
\end{aligned} \tag{80}$$

We also consider the "far–field" of ϕ_δ:

$$\psi_\delta(x_1) \;:=\; \sum_{n_1\neq 0}(-1)^{n_1}\,\ln\frac{1}{((x_1-n_1)^2+\delta^2)^{\frac{1}{2}}}$$

and observe

$$\psi_\delta \text{ is smooth on } (-\tfrac{1}{2},\tfrac{1}{2}) \text{ uniformly in } \delta \quad\text{and}\quad \frac{d\psi_\delta}{dx_1}(0) \;=\; 0.$$

Together with

$$\phi_\delta(0) \;\approx\; \tilde\phi_\delta(0) \;=\; \ln\frac{1}{\delta}, \tag{81}$$

we obtain

$$\left|\frac{\frac{d\psi_\delta}{dx_1}}{\phi_\delta(0)}\right| \lesssim (\ln^{-1}\frac{1}{\delta})\,\frac{|x_1|}{x_1^2+\delta^2} = |\frac{d\tilde{m}_1}{dx_1}|.$$

We conclude

$$(\frac{dm_1}{dx_1})^2 \sim (\frac{d\tilde{m}_1}{dx_1})^2 \quad \text{on} \quad (-\frac{1}{2},\frac{1}{2}). \tag{82}$$

Likewise, we have

$$|\psi_\delta(0)-\psi_\delta(x_1)| \ll \ln(1+(\frac{x_1}{\delta})^2) = \tilde{\phi}_\delta(0)-\tilde{\phi}_\delta(x_1) \quad \text{for } x_1\in(-\frac{1}{2},\frac{1}{2})$$

and thus

$$\phi_\delta(0)-\phi_\delta(x_1) \approx \tilde{\phi}_\delta(0)-\tilde{\phi}_\delta(x_1) \quad \text{for } x_1\in(-\frac{1}{2},\frac{1}{2}),$$

which together with (81) yields

$$1-m_1 \approx 1-\tilde{m}_1 \quad \text{or} \quad \frac{1}{1-m_1^2} \sim \frac{1}{1-\tilde{m}_1^2} \quad \text{on} \quad (-\frac{1}{2},\frac{1}{2}). \tag{83}$$

(82) and (83) combine into

$$\frac{1}{1-m_1^2}(\frac{dm_1}{dx_1})^2 \sim \frac{1}{1-\tilde{m}_1^2}(\frac{d\tilde{m}_1}{dx_1})^2 \quad \text{on} \quad (-\frac{1}{2},\frac{1}{2}).$$

Hence in view of the symmetry $m_1(x_1+1)=-m_1(x_1)$, (76) will follow from

$$\epsilon\int_{-1}^{1}\frac{1}{1-\tilde{m}_1^2}(\frac{d\tilde{m}_1}{dx_1})^2\,dx_1 \lesssim \frac{\epsilon}{\delta}\ln^{-1}\frac{1}{\delta}. \tag{84}$$

Let us now establish (84). We observe that

$$\tilde{m}_1(x_1) = \frac{\ln(x_1^2+\delta^2)}{\ln\delta^2} = 1-\frac{1}{2}(\ln^{-1}\frac{1}{\delta})\ln((\frac{x_1}{\delta})^2+1).$$

We thus have

$$\frac{1}{1-\tilde{m}_1^2}(\frac{d\tilde{m}_1}{dx_1})^2 \le \frac{1}{1-\tilde{m}_1}(\frac{d\tilde{m}_1}{dx_1})^2 = 2(\ln^{-1}\frac{1}{\delta})\frac{1}{\ln((\frac{x_1}{\delta})^2+1)}\frac{x_1^2}{(x_1^2+\delta^2)^2},$$

and hence as desired

$$\epsilon\int_{-\infty}^{\infty}\frac{1}{1-\tilde{m}_1^2}(\frac{d\tilde{m}_1}{dx_1})^2\,dx_1 \le \frac{\epsilon}{\delta}(\ln^{-1}\frac{1}{\delta})\int_{-\infty}^{\infty}\frac{2}{\ln(\hat{x}_1^2+1)}\frac{\hat{x}_1^2}{(\hat{x}_1^2+1)^2}\,d\hat{x}_1.$$

It remains to choose $\delta\ge\epsilon$. To this purpose, we observe that (76) and (77) yield

$$E_{thin}(m_1)-\pi\ln^{-1}\frac{1}{\delta} \lesssim \frac{\epsilon}{\delta}\ln^{-1}\frac{1}{\delta}+\ln^{-2}\frac{1}{\delta},$$

which we write as

$$(\ln\frac{1}{\epsilon})\,E_{thin}(m_1)\;-\;\pi\;\overset{\delta\geq\epsilon}{\lesssim}\;\frac{\epsilon}{\delta}\,\frac{\ln\frac{1}{\epsilon}}{\ln\frac{1}{\delta}}+\frac{\ln\frac{1}{\epsilon}}{\ln^2\frac{1}{\delta}}+\left(\frac{\ln\frac{1}{\epsilon}}{\ln\frac{1}{\delta}}-1\right). \tag{85}$$

We now see that

$$\delta\;=\;\epsilon\,\ln\frac{1}{\epsilon}$$

is a good choice. Indeed, we then have

$$\ln\frac{1}{\delta}\;=\;\ln\frac{1}{\epsilon}-\ln\ln\frac{1}{\epsilon}\;\overset{\epsilon\ll 1}{\approx}\;\ln\frac{1}{\epsilon}$$

and thus for each term appearing in the r. h. s. of (85)

$$\begin{aligned}
\frac{\epsilon}{\delta}\,\frac{\ln\frac{1}{\epsilon}}{\ln\frac{1}{\delta}}\;&=\;\frac{1}{\ln\frac{1}{\delta}}\;\approx\;\frac{1}{\ln\frac{1}{\epsilon}}\;\overset{\epsilon\ll 1}{\ll}\;\frac{\ln\ln\frac{1}{\epsilon}}{\ln\frac{1}{\epsilon}},\\
\frac{\ln\frac{1}{\epsilon}}{\ln^2\frac{1}{\delta}}\;&\approx\;\frac{1}{\ln\frac{1}{\epsilon}}\;\ll\;\frac{\ln\ln\frac{1}{\epsilon}}{\ln\frac{1}{\epsilon}},\\
\frac{\ln\frac{1}{\epsilon}}{\ln\frac{1}{\delta}}-1\;&=\;\frac{\ln\ln\frac{1}{\epsilon}}{\ln\frac{1}{\delta}}\;\approx\;\frac{\ln\ln\frac{1}{\epsilon}}{\ln\frac{1}{\epsilon}}.
\end{aligned}$$

□

Proof of Lemma 4.
We will drop the subscript 1 in the sequel. Our starting point is the explicit Fourier representation of m^* and ϕ_0 from Lemma 1 resp. Lemma 2. We immediately see that

$$u\;:=\;\phi_0-\lambda^*\,m^*$$

has the Fourier coefficients

$$u_n\;=\;\left\{\begin{array}{ll}\frac{\sqrt{2}}{|n|}-\frac{\sqrt{2}}{2\,\pi\,\epsilon\,n^2+|n|}\;=\;\sqrt{2}\,\frac{2\,\pi\,\epsilon}{2\,\pi\,\epsilon\,|n|+1} & \text{for } n \text{ odd}\\ 0 & \text{for } n \text{ even}\end{array}\right\}.$$

Therefore we have

$$u(x)\;=\;\sum_{n\,odd}\frac{2\,\pi\,\epsilon}{2\,\pi\,\epsilon\,|n|+1}\,e^{i\,\pi\,n\,x}\;=\;2\sum_{n\geq 1\,odd}\frac{2\,\pi\,\epsilon}{2\,\pi\,\epsilon\,n+1}\,\cos(\pi\,n\,x).$$

If we had a Fourier transform representation of u (instead of the discrete Fourier series representation), we would obtain the desired decay through integration by parts. We mimic this in our discrete setting:

$$\begin{aligned}
u(x)\;&=\;\frac{1}{\sin(\pi\,x)}\sum_{n\geq 1\,odd}\frac{2\,\pi\,\epsilon}{2\,\pi\,\epsilon\,n+1}\,\left(\sin(\pi\,(n+1)\,x)-\sin(\pi\,(n-1)\,x)\right)\\
&=\;\frac{1}{\sin(\pi\,x)}\sum_{n\geq 2\,even}\left(\frac{2\,\pi\,\epsilon}{2\,\pi\,\epsilon\,(n-1)+1}-\frac{2\,\pi\,\epsilon}{2\,\pi\,\epsilon\,(n+1)+1}\right)\,\sin(\pi\,n\,x)
\end{aligned}$$

$$
\begin{aligned}
&= \frac{2}{\sin(\pi\,x)} \sum_{n\geq 2\,even} \frac{(2\,\pi\,\epsilon)^2}{(2\,\pi\,\epsilon\,(n-1)+1)\,(2\,\pi\,\epsilon\,(n+1)+1)}\,\sin(\pi\,n\,x)\\
&= -\frac{1}{\sin^2(\pi\,x)} \sum_{n\geq 2\,even} \frac{(2\,\pi\,\epsilon)^2}{(2\,\pi\,\epsilon\,(n-1)+1)\,(2\,\pi\,\epsilon\,(n+1)+1)}\\
&\qquad \times \left(\cos(\pi\,(n+1)\,x) - \cos(\pi\,(n-1)\,x)\right)\\
&= \frac{\cos(\pi\,x)}{\sin^2(\pi\,x)}\,\frac{(2\,\pi\,\epsilon)^2}{(2\,\pi\,\epsilon+1)\,(2\,\pi\,\epsilon\,3+1)}\\
&\quad + \frac{1}{\sin^2(\pi\,x)} \sum_{n\geq 3\,odd} \left(\frac{(2\,\pi\,\epsilon)^2}{(2\,\pi\,\epsilon\,n+1)\,(2\,\pi\,\epsilon\,(n+2)+1)} - \frac{(2\,\pi\,\epsilon)^2}{(2\,\pi\,\epsilon\,(n-2)+1)\,(2\,\pi\,\epsilon\,n+1)}\right)\\
&\qquad \times \cos(\pi\,n\,x)\\
&= \frac{\cos(\pi\,x)}{\sin^2(\pi\,x)}\,\frac{(2\,\pi\,\epsilon)^2}{(2\,\pi\,\epsilon+1)\,(2\,\pi\,\epsilon\,3+1)}\\
&\quad - \frac{(2\,\pi\,\epsilon)^3}{\sin^2(\pi\,x)} \sum_{n\geq 3\,odd} \frac{4}{(2\,\pi\,\epsilon\,n+1)\,(2\,\pi\,\epsilon\,(n+2)+1)\,(2\,\pi\,\epsilon\,(n-2)+1)}\,\cos(\pi\,n\,x)\\
&\approx \left(\frac{2\,\pi\,\epsilon}{\sin(\pi\,x)}\right)^2 \cos(\pi\,x).
\end{aligned}
$$

In particular, we obtain

$$
|u(x)| \;\lesssim\; \left(\frac{2\,\pi\,\epsilon}{\sin(\pi\,x)}\right)^2
$$

and thus as desired

$$
|u(x)| \;\lesssim\; \left(\frac{\epsilon}{x}\right)^2 \quad \text{for } |x| \ll 1.
$$

□

Proof of Lemma 5.
From Lemma 1 we know

$$
|\tilde{E}_{thin}(m_1^*) - \pi\,\ln^{-1}\frac{1}{\epsilon}| \;\lesssim\; \frac{1}{\ln^2\frac{1}{\epsilon}}.
$$

Together with the upper bound in Lemma 3, i. e.

$$
E_{thin}(m_1) - \pi\,\ln^{-1}\frac{1}{\epsilon} \;\lesssim\; \frac{\ln\ln\frac{1}{\epsilon}}{\ln^2\frac{1}{\epsilon}},
$$

we obtain from the decomposition (61) that in particular

$$
\epsilon\int_{-1}^{1}(\frac{d\zeta_1}{dx_1})^2\,dx_1 \;\leq\; \tilde{E}_{thin}(\zeta_1) \;\lesssim\; \frac{\ln\ln\frac{1}{\epsilon}}{\ln^2\frac{1}{\epsilon}}.
$$

Since $\zeta_1(0) = 0$ (c. f. (60)), we have

$$
|\zeta_1(x_1)| \;\leq\; \left|\int_0^{x_1} |\frac{d\zeta_1}{dy_1}|\,dy_1\right| \;\leq\; \left(|x_1|\int_{-1}^{1}(\frac{d\zeta_1}{dy_1})^2\,dy_1\right)^{\frac{1}{2}} \;\lesssim\; \frac{1}{\ln\frac{1}{\epsilon}}\left(\frac{|x_1|}{\epsilon}\ln\ln\frac{1}{\epsilon}\right)^{\frac{1}{2}}.
$$

Now δ is defined in (62) such that

$$|\zeta_1(x_1)| \;\lesssim\; \frac{1}{\ln\frac{1}{\epsilon}}\left(\frac{\delta}{\epsilon}\ln\ln\frac{1}{\epsilon}\right)^{\frac{1}{2}} \;=\; \frac{\epsilon}{\delta} \quad \text{for } |x_1|\le\delta. \tag{86}$$

Let us write

$$\begin{aligned}
&1-m_1^* \\
&\quad= \left(1-\ln^{-1}\frac{1}{\epsilon}\,\ln\frac{1}{|x_1|}\right) + (\ln^{-1}\frac{1}{\epsilon})\,(\ln\frac{1}{|x_1|}-\lambda^*\,m_1^*) + ((\ln^{-1}\frac{1}{\epsilon})\lambda^*-1)\,m_1^* \\
&\quad= \frac{\ln\frac{|x_1|}{\epsilon}}{\ln\frac{1}{\epsilon}} + (\ln^{-1}\frac{1}{\epsilon})\,(\ln\frac{1}{|x_1|}-\lambda^*\,m_1^*) + ((\ln^{-1}\frac{1}{\epsilon})\lambda^*-1)\,m_1^* \\
&\quad=: T_1+T_2+T_3.
\end{aligned}$$

For T_1 we observe that

$$|T_1| \;\le\; (\ln^{-1}\frac{1}{\epsilon})\,\ln\frac{\delta}{\epsilon} \;\lesssim\; \frac{\ln\ln\frac{1}{\epsilon}}{\ln\frac{1}{\epsilon}} \quad \text{for } \epsilon\le|x_1|\le\delta.$$

We bound T_2 with help of Lemma 4

$$|T_2| \;\lesssim\; (\ln^{-1}\frac{1}{\epsilon})\left(|\phi_0(x_1)-\ln\frac{1}{|x_1|}| + (\frac{\epsilon}{|x_1|})^2\right) \;\le\; \ln^{-1}\frac{1}{\epsilon} \;\ll\; \frac{\ln\ln\frac{1}{\epsilon}}{\ln\frac{1}{\epsilon}} \quad \text{for } \epsilon\le|x_1|\le\delta.$$

According to (54) we have

$$|T_3| \;\lesssim\; \ln^{-1}\frac{1}{\epsilon} \;\ll\; \frac{\ln\ln\frac{1}{\epsilon}}{\ln\frac{1}{\epsilon}}.$$

Hence we obtain

$$|1-m_1^*| \;\lesssim\; \frac{\ln\ln\frac{1}{\epsilon}}{\ln\frac{1}{\epsilon}} \;\ll\; \frac{(\ln\ln\frac{1}{\epsilon})^{\frac{1}{3}}}{\ln^{\frac{2}{3}}\frac{1}{\epsilon}} \;=\; \frac{\epsilon}{\delta} \quad \text{for } \epsilon\le|x_1|\le\delta. \tag{87}$$

Combining (86) and (87), we obtain for $m_1 = m_1^*+\zeta_1$

$$|1-m_1| \;\lesssim\; \frac{\epsilon}{\delta} \quad \text{for } \epsilon\le|x_1|\le\delta.$$

resp.

$$\frac{m_1^2}{1-m_1^2} \;\gtrsim\; \frac{\delta}{\epsilon} \quad \text{for } \epsilon\le|x_1|\le\delta.$$

This yields (63). □

Proof of Lemma 6.

Let $C < \infty$ denote a generic universal constant. We extend ζ harmonically onto $(x_1, x_3) \in I\!R^2$ so that we have

$$\sum_{n_1} \frac{\pi\,|n_1|}{2}\,|\zeta_{1,n_1}|^2 \;=\; \frac{1}{4}\int_{-1}^{1}\int_{-\infty}^{\infty}(\frac{\partial\zeta}{\partial x_1})^2+(\frac{\partial\zeta}{\partial x_3})^2\,dx_3\,dx_1. \tag{88}$$

By the trace theorem and a scaling argument, we have

$$C\int_{2^{-(k+1)}}^{2^{-k}}\int_{-2^{-(k+1)}}^{2^{-(k+1)}}(\frac{\partial\zeta}{\partial x_1})^2+(\frac{\partial\zeta}{\partial x_3})^2\,dx_3\,dx_1 \;\geq\; 2^k\int_{2^{-(k+1)}}^{2^{-k}}(\zeta-\bar\zeta)^2\,dx_1, \tag{89}$$

where $\bar\zeta$ denotes the mean value of ζ on the x_1–interval $(2^{-(k+1)}, 2^{-k})$. Likewise, we have by Poincaré's estimate and a scaling argument

$$\begin{aligned}
&C\int_{2^{-(k+1)}}^{2^{-k}}(\frac{d}{dx_1}(\zeta-u))^2\,dx_1\\
&\quad\geq\; (2^k)^2\int_{2^{-(k+1)}}^{2^{-k}}\Big((\zeta-u)-\overline{(\zeta-u)}\Big)^2\,dx_1\\
&\quad\geq\; (2^k)^2\left(\left(\int_{2^{-(k+1)}}^{2^{-k}}(u-\bar u)^2\,dx_1\right)^{\frac12}-\left(\int_{2^{-(k+1)}}^{2^{-k}}(\zeta-\bar\zeta)^2\,dx_1\right)^{\frac12}\right)^2.
\end{aligned}\tag{90}$$

Now (89), (90) and our assumption (65) combine into

$$\begin{aligned}
&C\Big\{\int_{2^{-(k+1)}}^{2^{-k}}\int_{-2^{-(k+1)}}^{2^{-(k+1)}}(\frac{\partial\zeta}{\partial x_1})^2+(\frac{\partial\zeta}{\partial x_3})^2\,dx_3\,dx_1\\
&\qquad +2^{-k}\int_{2^{-(k+1)}}^{2^{-k}}(\frac{d}{dx_1}(\zeta-u))^2\,dx_1\Big\}\\
&\quad\geq\; 2^k\Big\{\int_{2^{-(k+1)}}^{2^{-k}}(\zeta-\bar\zeta)^2\,dx_1\\
&\qquad +\left(\left(\int_{2^{-(k+1)}}^{2^{-k}}(u-\bar u)^2\,dx_1\right)^{\frac12}-\left(\int_{2^{-(k+1)}}^{2^{-k}}(\zeta-\bar\zeta)^2\,dx_1\right)^{\frac12}\right)^2\Big\}\\
&\quad\geq\; 2^k\,\frac12\int_{2^{-(k+1)}}^{2^{-k}}(u-\bar u)^2\,dx_1\;\gtrsim\;1,
\end{aligned}$$

provided $\epsilon \ll 2^{-k} \ll \delta$. Given two nonnegative integers $k_{min} \ll k_{max}$, we sum this estimate over $k \in \{k_{min}, \ldots, k_{max}\}$ and use (88)

$$\begin{aligned}
&\sum_{n_1}\frac{\pi\,|n_1|}{2}\,|\zeta_{1,n_1}|^2+2^{-k_{min}}\int_{2^{-k_{max}+1}}^{2^{-k_{min}}}(\frac{d}{dx_1}(\zeta-u))^2\,dx_1\\
&\quad\gtrsim\;\int_{2^{-(k_{max}+1)}}^{2^{-k_{min}}}\int_{-\infty}^{\infty}(\frac{\partial\zeta}{\partial x_1})^2+(\frac{\partial\zeta}{\partial x_3})^2\,dx_3\,dx_1+2^{-k_{min}}\int_{2^{-(k_{max}+1)}}^{2^{-k_{min}}}(\frac{d}{dx_1}(\zeta-u))^2\,dx_1\\
&\quad\gtrsim\;\sum_{k=k_{min}}^{k_{max}}\Big\{\int_{2^{-(k+1)}}^{2^{-k}}\int_{-2^{-(k+1)}}^{2^{-(k+1)}}(\frac{\partial\zeta}{\partial x_1})^2+(\frac{\partial\zeta}{\partial x_3})^2\,dx_3\,dx_1\\
&\qquad +\;2^{-k}\int_{2^{-(k+1)}}^{2^{-k}}(\frac{d}{dx_1}(\zeta-u))^2\,dx_1\Big\}\\
&\quad\gtrsim\;k_{max}-k_{min}+1\;\sim\;\ln\frac{2^{-k_{min}}}{2^{-(k_{max}+1)}}.
\end{aligned}$$

It remains to choose the two nonnegative integers $k_{min} \ll k_{max}$ such that

$$2^{-k_{min}} \sim \delta \quad \text{and} \quad 2^{-(k_{max}+1)} \sim \epsilon,$$

which is possible according to (64). □

Proof of Lemma 7.
According to (61) and (63), we have

$$\begin{aligned}
&E_{thin}(m_1) - \tilde{E}_{thin}(m_1^*) \\
&\quad = \tilde{E}_{thin}(\zeta_1) + \epsilon \int_{-1}^{1} \frac{m_1^2}{1-m_1^2} (\frac{dm_1}{dx_1})^2 \, dx_1 \\
&\quad \geq \sum_{n_1} \frac{\pi \, |n_1|}{2} \, |\zeta_{1,n_1}|^2 + \delta \int_{\epsilon}^{\delta} (\frac{dm_1}{dx_1})^2 \, dx_1 \\
&\quad = \ln^{-2} \frac{1}{\epsilon} \Big\{ \sum_{n_1} \frac{\pi \, |n_1|}{2} \, |(\ln \frac{1}{\epsilon}) \, \zeta_{1,n_1}|^2 \\
&\qquad + \delta \int_{\epsilon}^{\delta} \left(\frac{d}{dx_1} \left((\ln \frac{1}{\epsilon}) \, \zeta_1 + (\ln \frac{1}{\epsilon}) \, m_1^* \right) \right)^2 \, dx_1 \Big\}. \qquad (91)
\end{aligned}$$

We now wish to apply Lemma 6 to

$$\zeta := (\ln \frac{1}{\epsilon}) \, \zeta_1 \quad \text{and} \quad u := -(\ln \frac{1}{\epsilon}) \, m_1^*.$$

We have to verify (65). Since according to (54), $\lambda^* \approx \ln \frac{1}{\epsilon}$, we have to show that

$$\int_{\alpha}^{2\,\alpha} (\lambda^* \, m_1^* - \overline{\lambda^* \, m_1^*})^2 \, dx_1 \gtrsim \alpha \quad \text{for all } \epsilon \ll \alpha \ll \delta. \qquad (92)$$

Indeed, we have on one hand according to Lemma 4 that $\lambda^* \, m_1^*$ is close to ϕ_0 in the sense of

$$\begin{aligned}
\Big| \left(\int_{\alpha}^{2\,\alpha} (\lambda^* \, m_1^* - \overline{\lambda^* \, m_1^*})^2 \, dx_1 \right)^{\frac{1}{2}} \; &- \; \left(\int_{\alpha}^{2\,\alpha} \left(\ln \frac{1}{|x_1|} - \tfrac{1}{\alpha} \int_{\alpha}^{2\,\alpha} \ln \frac{1}{|y_1|} \, dy_1 \right)^2 \, dx_1 \right)^{\frac{1}{2}} \Big| \\
&\lesssim \left(\int_{\alpha}^{2\,\alpha} (\frac{\epsilon}{x_1})^2 \, dx_1 \right)^{\frac{1}{2}} \sim \frac{\epsilon}{\sqrt{\alpha}} \ll \sqrt{\alpha}. \qquad (93)
\end{aligned}$$

On the other hand, ϕ_0 is close to $\log \frac{1}{|x_1|}$ and we thus have the well–known property of the logarithm $\log \frac{1}{|x_1|}$

$$\begin{aligned}
\int_{\alpha}^{2\,\alpha} \left(\phi_0(x_1) - \frac{1}{\alpha} \int_{\alpha}^{2\,\alpha} \phi_0(y_1) \, dy_1 \right)^2 \, dx_1 \; &\approx \; \int_{\alpha}^{2\,\alpha} \left(\ln \frac{1}{|x_1|} - \frac{1}{\alpha} \int_{\alpha}^{2\,\alpha} \ln \frac{1}{|y_1|} \, dy_1 \right)^2 \, dx_1 \\
&= \int_{\alpha}^{2\,\alpha} \left(\frac{1}{\alpha} \int_{\alpha}^{2\,\alpha} \ln \frac{|x_1|}{|y_1|} \, dy_1 \right)^2 \, dx_1 \\
&= \alpha \int_{1}^{2} \left(\int_{1}^{2} \ln \frac{|\hat{x}_1|}{|\hat{y}_1|} \, d\hat{y}_1 \right)^2 \, d\hat{x}_1 \\
&\sim \alpha. \qquad (94)
\end{aligned}$$

The estimate (92) now follows from (93) and (94). Hence the application of Lemma 6 on the l. h. s. of (91) yields as desired

$$E_{thin}(m_1) - \tilde{E}_{thin}(m_1^*) \;\gtrsim\; (\ln^{-2}\frac{1}{\epsilon})\,\ln\frac{\delta}{\epsilon} \;\overset{(62)}{\sim}\; \frac{\ln\ln\frac{1}{\epsilon}}{\ln^2\frac{1}{\epsilon}}.$$

□

5.3 Proof of Theorem 1

We pass to the same reduced variables as in Proposition 1:

$$x_1 \;=\; d\,\hat{x}_1 \quad\text{and}\quad E \;=\; d\,t\,\hat{E}.$$

Then

$$\hat{E}(m') \;=\; \int_{-\hat{w}}^{\hat{w}} |\frac{dm'}{d\hat{x}_1}|^2\,d\hat{x}_1 + \sum_{\hat{n}_1} f(\frac{\pi\,\hat{t}\,|\hat{n}_1|}{2\,\hat{w}})|m_{1,\hat{n}_1}|^2,$$

where $m_{1,\hat{n}_1}$ denote the Fourier coefficients

$$m_{1,\hat{n}_1} \;=\; \frac{1}{(2\,\hat{w})^{\frac{1}{2}}}\int_{-\hat{w}}^{\hat{w}} e^{i\,\pi\,\hat{n}_1\,\frac{\hat{x}_1}{\hat{w}}}\,m_1(\hat{x}_1)\,d\hat{x}_1$$

and where — as opposed to Proposition 1 — there are *two* non–dimensional parameters $\hat{w}$ and $\hat{t}$ which according to (30) satisfy

$$\hat{w} \;:=\; \frac{w}{d} \;\gg\; 1 \quad\text{and}\quad \ln\hat{w} \;\ll\; \hat{t} \;:=\; \frac{t}{d} \;\ll\; \hat{w}. \tag{95}$$

Our goal is to show that in the regime (95),

$$\min_{m'}\hat{E}(m') - 8 \;\approx\; -4\,\pi\,\frac{1}{\hat{t}}\,\ln\hat{w}, \tag{96}$$

where the minimum is taken over all m' of the form (10) with

$$\theta(\hat{x}_1 + \hat{w}) \;=\; \theta(\hat{x}_1) + \pi.$$

In the sequel, we will drop the hats.

The natural strategy is to write the variational problem (96) as a perturbation of its thick–film approximation (37). More precisely, we will view

- m as a perturbation of the minimizer m^* of the thick–film approximation (normalized by $\theta^*(0) = 0$),
- E as a perturbation of E_{thick}.

For the latter we observe that in view of $f = 1 - g$, we have

$$E(m') \;=\; E_{thick}(m') \;-\; \sum_{n_1} g(\frac{\pi\, t\, |n_1|}{2\, w})|m_{1,n_1}|^2, \tag{97}$$

where g is defined in (7). As in Proposition 2, it will be convenient to express the exchange energy in terms of m_1 alone

$$\int_{-w}^{w} |\frac{dm'}{dx_1}|^2\, dx_1 \;=\; \int_{-w}^{w} \phi(\frac{dm_1}{dx_1}, m_1)\, dx_1,$$

where

$$\phi(p, m) \;:=\; \frac{1}{1 - m^2}\, p^2.$$

Therefore the Euler–Lagrange equation for m_1^* can be written in terms of

$$\begin{aligned}
&\langle \mathrm{grad} E_{thick}(m_1^*), \zeta_1 \rangle \\
&\quad = \int_{-w}^{w} \left\{ \partial_p \phi(\frac{dm_1^*}{dx_1}, m_1^*)\, \frac{d\zeta_1}{dx_1} + \partial_m \phi(\frac{dm_1^*}{dx_1}, m_1^*)\, \zeta_1 \right\} dx_1 \;+\; 2 \int_{-w}^{w} m_1^*\, \zeta_1\, dx_1 \;=\; 0.
\end{aligned}$$

We will use the Euler–Lagrange equation in the following form

$$\begin{aligned}
&E_{thick}(m_1) - E_{thick}(m_1^*) \\
&\quad = \int_{-w}^{w} \Big\{ \phi(\frac{dm_1}{dx_1}, m_1) - \phi(\frac{dm_1^*}{dx_1}, m_1^*) \\
&\qquad\qquad -\partial_p \phi(\frac{dm_1^*}{dx_1}, m_1^*)\, \frac{d\zeta_1}{dx_1} - \partial_m \phi(\frac{dm_1^*}{dx_1}, m_1^*)\, \zeta_1 \Big\}\, dx_1 \;+\; \int_{-w}^{w} \zeta_1^2\, dx_1,
\end{aligned} \tag{98}$$

where

$$\zeta_1 \;=\; m_1 - m_1^*.$$

We now split the energy into four parts

$$\begin{aligned}
&E(m) \\
&\quad \overset{(97)}{=}\; E_{thick}(m_1) - \sum_{n_1} g(\frac{\pi\, t\, |n_1|}{2\, w})|m_{1,n_1}|^2 \\
&\quad = \; E_{thick}(m_1^*) \;+\; (E_{thick}(m_1) - E_{thick}(m_1^*)) - \sum_{n_1} g(\frac{\pi\, t\, |n_1|}{2\, w})|m_{1,n_1}|^2 \\
&\quad \overset{(98)}{=}\; E_{thick}(m_1^*) \\
&\quad + \int_{-w}^{w} \Big\{ \phi(\frac{dm_1}{dx_1}, m_1) - \phi(\frac{dm_1^*}{dx_1}, m_1^*) \\
&\qquad\qquad -\partial_p \phi(\frac{dm_1^*}{dx_1}, m_1^*)\, \frac{d\zeta_1}{dx_1} - \partial_m \phi(\frac{dm_1^*}{dx_1}, m_1^*)\, \zeta_1 \Big\}\, dx_1 \\
&\quad + \int_{-w}^{w} \zeta_1^2\, dx_1
\end{aligned}$$

$$
\begin{aligned}
&- \sum_{n_1} g(\frac{\pi\, t\, |n_1|}{2\, w})|m^*_{1,n_1}|^2 - 2 \sum_{n_1} g(\frac{\pi\, t\, |n_1|}{2\, w})\mathrm{Re}(\zeta_{1,n_1}\, \overline{m^*_{1,n_1}}) - \sum_{n_1} g(\frac{\pi\, t\, |n_1|}{2\, w})|\zeta_{1,n_1}|^2 \\
&\stackrel{f=1-g}{=} E_{thick}(m^*_1) \\
&- \sum_{n_1} g(\frac{\pi\, t\, |n_1|}{2\, w})|m^*_{1,n_1}|^2 \\
&+ \int_{-w}^{w} \Big\{ \phi(\frac{dm_1}{dx_1}, m_1) - \phi(\frac{dm^*_1}{dx_1}, m^*_1) \\
&\qquad -\partial_p \phi(\frac{dm^*_1}{dx_1}, m^*_1)\, \frac{d\zeta_1}{dx_1} - \partial_m \phi(\frac{dm^*_1}{dx_1}, m^*_1)\, \zeta_1 \Big\}\, dx_1 \\
&+ \sum_{n_1} f(\frac{\pi\, t\, |n_1|}{2\, w})|\zeta_{1,n_1}|^2 - 2 \sum_{n_1} g(\frac{\pi\, t\, |n_1|}{2\, w})\mathrm{Re}(\zeta_{1,n_1}\, \overline{m^*_{1,n_1}}) \\
&=: T_1 \;+\; T_2 \;+\; T_3 \;+\; T_4.
\end{aligned}
$$

We will show that the leading order term comes from T_1, the first order correction from T_4 and that T_2 and T_3 are higher order. More precisely: In Proposition 1, we have shown

$$
T_1 - 8 \;\sim\; \exp(-w) \;\stackrel{(95)}{\ll}\; \frac{1}{t} \ln w.
$$

In Lemma 10 we shall establish

$$
0 \;\leq\; -T_2 \;\lesssim\; \frac{1}{t} \ln t \;\stackrel{(95)}{\ll}\; \frac{1}{t} \ln w.
$$

It will follow from Lemma 8 that

$$
T_3 \;\geq\; 0.
$$

We will show in Lemma 11 that

$$
T_4 \;\gtrapprox\; -4\, \pi\, \frac{1}{t} \ln w,
$$

for any ζ_1 with the symmetry $\zeta_1(x_1 + w) \;=\; -\zeta(x_1)$. This yields the lower half of (96):

$$
\min_{m'} E(m') - 8 \;\gtrapprox\; -4\, \pi\, \frac{1}{t} \ln w.
$$

In Lemma 12 and Lemma 13 we will construct a ζ_1 with the symmetry $\zeta_1(x_1 + w) = -\zeta_1(x_1)$, $\zeta_1(0) = 0$, s. t.

$$
T_3 \;\lesssim\; (\frac{\ln w}{t})^2 \stackrel{(95)}{\ll} \frac{1}{t} \ln w
$$

and

$$
T_4 \;\lessapprox\; -4\, \pi\, \frac{1}{t} \ln w.
$$

This yields the upper half of (96). We now state and prove the lemmas. In the sequel, we will drop the subscript "1".

Lemma 8 establishes a convexity property for the exchange energy integrand, which is very useful for the lower bound.

Lemma 8 *We have*

$$\begin{aligned} 0 \;&\leq\; \phi(p,m) - \phi(p^*,m^*) - \partial_p\phi(p^*,m^*)\,(p-p^*) - \partial_m\phi(p^*,m^*)\,(m-m^*) \\ &\leq\; 2\max\left\{\frac{1}{1-m^2}\,,\,\frac{1}{1-(m^*)^2}\right\}(p-p^*)^2 \\ &\quad + 8\max\left\{\frac{1}{1-m^2}\,,\,\frac{1}{1-(m^*)^2}\right\}^3 \max\left\{p^2,(p^*)^2\right\}\,(m-m^*)^2. \end{aligned}$$

Lemma 9 collects all the relevant properties of the thick–film Néel wall.

Lemma 9 *Consider the minimizer $m^* = \cos\theta^*$ of E_{thick} among all θ with $\theta(x+w) = \theta(x)+\pi$, normalized by $\theta^*(0) = 0$. It satisfies*

i)

$$m^* \;=\; \cos\theta^* \;\geq\; 0 \quad in \quad (-\frac{w}{2},\frac{w}{2})$$

ii)

$$\int_{-\frac{w}{2}}^{\frac{w}{2}} m^*\,dx \;\left\{\begin{array}{c}\leq\\ \approx\end{array}\right\}\; \pi, \qquad \int_{-\frac{w}{2}}^{\frac{w}{2}} |x|\,m^*\,dx \;\sim\; 1$$

iii)

$$m_n^* \;\approx\; (\frac{2}{w})^{\frac{1}{2}}\,\pi \quad for\ all\ odd\ n\ with\ |n| \ll w, \qquad |m_n^*| \;\leq\; (\frac{2}{w})^{\frac{1}{2}}\,\pi$$

iv)

$$\left.\begin{array}{rcl} 1-m^* & \approx & \frac{1}{2}\,x^2 \\ \frac{dm^*}{dx} & \approx & x \end{array}\right\} \quad for\ |x| \ll 1$$

v)

$$m^* \;\lesssim\; \exp(-|x|) \quad for\ 1 \ll |x| \;\leq\; \frac{w}{2}$$

Lemma 10 shows that the true stray–field energy of the thick–film Néel wall m^* deviates from its thick–film approximation by a term of lower order.

Lemma 10

$$\sum_n g\left(\frac{\pi\,|n|\,t}{2\,w}\right)\,|m_n^*|^2 \;\lesssim\; \frac{1}{t}\,\ln t.$$

Lemma 11 bounds by below the correction in the stray–field energy due to a perturbation ζ of the thick–film Néll wall m^*. This yields the leading order in the correction.

Lemma 11

$$\sum_n f\left(\frac{\pi\,|n|\,t}{2\,w}\right)\,|\zeta_n|^2 \;-\; 2\sum_n g\left(\frac{\pi\,|n|\,t}{2\,w}\right)\,\mathrm{Re}(\zeta_n\,\overline{m_n^*}) \;\gtrapprox\; -4\,\pi\,\frac{1}{t}\,\ln w$$

for all ζ with $\zeta(x+w) = -\zeta(x)$.

We now introduce the upper bound construction $m = m^* + \zeta$. Consider ζ given by

$$\zeta_n \;=\; \frac{1}{t}\left\{\begin{array}{lllll} \dfrac{(8\,w)^{\frac{1}{2}}}{|n|} & \text{for} & & |n| & \leq \dfrac{w}{t} \\ 0 & \text{for} & \dfrac{w}{t} & < |n| & \leq w \\ -\lambda\,\dfrac{w^{\frac{7}{2}}\,\ln w}{|n|^4} & \text{for} & w & < |n| & \end{array}\right\} \quad \text{for } n \text{ odd}$$

and $\zeta_n \;=\; 0$ for n even, where λ is chosen s. t.

$$\sum_n \zeta_n \;=\; 0.$$

Lemma 12 shows that the upper bound construction ζ realizes the leading order correction of the stray–field energy from Lemma 11.

Lemma 12 *The above ζ has the symmetries*

$$\zeta(x+w) \;=\; -\zeta(x), \quad \zeta(x) \;\in\; I\!R \quad \textit{and} \quad \zeta(-x) \;=\; \zeta(x) \tag{99}$$

and satisfies

$$\sum_n f\left(\frac{\pi\,|n|\,t}{2\,w}\right)\,|\zeta_n|^2 \;-\; 2\sum_n g\left(\frac{\pi\,|n|\,t}{2\,w}\right)\,\mathrm{Re}(\zeta_n\,\overline{m_n^*}) \;\lessapprox\; -4\,\pi\,\frac{1}{t}\,\ln w.$$

In connection with Lemma 8, Lemma 13 shows that the correction in the exchange energy for our upper bound construction ζ is of higher order.

Lemma 13 *For the above ζ we have*

i)

$$\zeta(0) \;=\; 0, \qquad \frac{d\zeta}{dx}(0) \;=\; 0$$

ii)

$$\sup_{(-w,w)}\,|\zeta| \;+\; \sup_{(-w,w)}\,|\frac{d\zeta}{dx}| \;+\; \sup_{(-w,w)}\,|\frac{d^2\zeta}{dx^2}| \;\lesssim\; \frac{\ln w}{t}$$

iii)

$$\int_{-w}^{w}(\frac{d\zeta}{dx})^2\,dx \;\lesssim\; \left(\frac{\ln w}{t}\right)^2$$

iv) We have $|m| \leq 1$ and

$$\begin{aligned}\int_{-w}^{w} &\max\left\{\frac{1}{1-m^2}\,,\,\frac{1}{1-(m^*)^2}\right\}\,(\frac{d\zeta}{dx})^2 \\ &+\max\left\{\frac{1}{1-m^2},\frac{1}{1-(m^*)^2}\right\}^3\,\max\left\{(\frac{dm}{dx})^2\,,\,(\frac{dm^*}{dx})^2\right\}\,\zeta^2\,dx \\ &\lesssim\; \left(\frac{\ln w}{t}\right)^2 \quad \textit{where } m \;=\; m^*+\zeta.\end{aligned}$$

PROOF OF LEMMA 8

The first and second derivatives of ϕ are given by

$$\begin{aligned}
\partial_p \phi(p,m) &= \frac{2}{1-m^2}\, p, \\
\partial_m \phi(p,m) &= \frac{2\,m}{(1-m^2)^2}\, p^2, \\
\partial^2_{pp} \phi(p,m) &= \frac{2}{1-m^2}, \\
\partial^2_{pm} \phi(p,m) &= \frac{4\,m}{(1-m^2)^2}\, p, \\
\partial^2_{mm} \phi(p,m) &= \left(\frac{2}{(1-m^2)^2} + \frac{8\,m^2}{(1-m^2)^3} \right) p^2 \;=\; \frac{2+6\,m^2}{(1-m^2)^3}\, p^2.
\end{aligned}$$

Since

$$\partial^2_{pp} \phi \;\geq\; 0$$

and

$$\begin{aligned}
\det D^2 \phi &= \partial^2_{pp}\phi\, \partial^2_{mm}\phi - (\partial^2_{pm}\phi)^2 \\
&\geq \frac{2}{1-m^2}\, \frac{8\,m^2}{(1-m^2)^3}\, p^2 - \left(\frac{4\,m}{(1-m^2)^3}\, p \right)^2 \;=\; 0, \qquad (100)
\end{aligned}$$

the matrix $D^2\phi$ is positive semi–definite. Hence ϕ is convex. This establishes the first inequality of Lemma 8.

For the second inequality, we observe that

$$\begin{aligned}
\frac{1}{2} \begin{pmatrix} q \\ \zeta \end{pmatrix} \cdot D^2 \phi(p,m) \begin{pmatrix} q \\ \zeta \end{pmatrix} &\overset{(100)}{\leq} \partial^2_{pp}\phi(p,m)\, q^2 + \partial^2_{mm}\phi(p,m)\, \zeta^2 \\
&\leq \frac{2}{1-m^2}\, q^2 + \frac{8\,p^2}{(1-m^2)^3}\, \zeta^2
\end{aligned}$$

and

$$\begin{aligned}
\max_{t\in[0,1]} \left\{ \frac{1}{1-(t\,m+(1-t)\,m^*)^2} \right\} &\leq \max\left\{ \frac{1}{1-m^2}\,,\, \frac{1}{1-(m^*)^2} \right\}, \\
\max_{t\in[0,1]} \left\{ \frac{(t\,p+(1-t)\,p^*)^2}{(1-(t\,m+(1-t)\,m^*)^2)^3} \right\} &\leq \max\left\{ \frac{1}{1-m^2}\,,\, \frac{1}{1-(m^*)^2} \right\}^3 \\
&\quad \times \max\left\{ p^2, (p^*)^2 \right\}.
\end{aligned}$$

□

PROOF OF LEMMA 9: According to (39) and (40) in the proof of Proposition 1 we have the implicit formula for θ^*

$$\int_0^{\theta^*(x)} \frac{1}{(\cos^2\theta + \epsilon^2)^{\frac{1}{2}}}\, d\theta \;=\; x. \qquad (101)$$

Recall also that ϵ is implicitly determined by

$$\int_0^{\frac{\pi}{2}} \frac{1}{(\cos^2\theta+\epsilon^2)^{\frac{1}{2}}}\,d\theta \;=\; \frac{w}{2}, \tag{102}$$

and that

$$\epsilon \;\approx\; \exp(-\frac{w}{2}) \;\ll\; 1, \tag{103}$$

c. f. (42) and (45). In view of the monotonicity of θ^* (c. f. (41)), this implies

$$\theta^*((-\frac{w}{2},\frac{w}{2})) \;=\; (-\frac{\pi}{2},\frac{\pi}{2}), \tag{104}$$

which yields i).

We now tackle ii). We have

$$\begin{aligned}
\int_{-\frac{w}{2}}^{\frac{w}{2}} \cos\theta^*\,dx \qquad &\overset{(39)}{=} \qquad \int_{-\frac{w}{2}}^{\frac{w}{2}} \frac{\cos\theta^*}{(\cos^2\theta^*+\epsilon^2)^{\frac{1}{2}}}\,\frac{d\theta^*}{dx}\,dx \\
&\overset{(104)}{=} \qquad \int_{-\frac{\pi}{2}}^{\frac{\pi}{2}} \frac{\cos\theta}{(\cos^2\theta+\epsilon^2)^{\frac{1}{2}}}\,d\theta \\
&\left\{\begin{array}{c}\overset{(103)}{\approx}\\ \leq\end{array}\right\} \quad \int_{-\frac{\pi}{2}}^{\frac{\pi}{2}} 1\,d\theta \;=\; \pi.
\end{aligned}$$

Similarly,

$$\begin{aligned}
&\int_{-\frac{w}{2}}^{\frac{w}{2}} |x|\,\cos\theta^*\,dx \\
&\quad\overset{(101)}{=} \int_{-\frac{w}{2}}^{\frac{w}{2}} \left|\int_0^{\theta^*} \frac{1}{(\cos^2\varphi+\epsilon^2)^{\frac{1}{2}}}\,d\varphi\right| \cos\theta^*\,dx \\
&\quad\overset{(39)}{=} \int_{-\frac{w}{2}}^{\frac{w}{2}} \left|\int_0^{\theta^*} \frac{1}{(\cos^2\varphi+\epsilon^2)^{\frac{1}{2}}}\,d\varphi\right| \frac{\cos\theta^*}{(\cos^2\theta^*+\epsilon^2)^{\frac{1}{2}}}\,\frac{d\theta^*}{dx}\;dx \\
&\quad\overset{(104)}{=} \int_{-\frac{\pi}{2}}^{\frac{\pi}{2}} \left|\int_0^{\theta} \frac{1}{(\cos^2\varphi+\epsilon^2)^{\frac{1}{2}}}\,d\varphi\right| \frac{\cos\theta}{(\cos^2\theta+\epsilon^2)^{\frac{1}{2}}}\,d\theta \\
&\quad\overset{(103)}{\approx} \int_{-\frac{\pi}{2}}^{\frac{\pi}{2}} \left|\int_0^{\theta} \frac{1}{\cos\varphi}\,d\varphi\right| d\theta \\
&\quad= \;2\int_0^{\frac{\pi}{2}}\int_0^{\theta} \frac{1}{\cos\varphi}\,d\varphi\,d\theta \\
&\quad= \;2\int_0^{\frac{\pi}{2}} (\frac{\pi}{2}-\varphi)\,\frac{1}{\cos\varphi}\,d\varphi \;\sim\; 1.
\end{aligned}$$

From ii) we now infer the statements iii) on the Fourier coefficients

$$m_n^* \;=\; \frac{1}{(2w)^{\frac{1}{2}}}\int_{-w}^{w} e^{i\,\pi\,n\,\frac{x}{w}}\,m^*(x)\,dx$$

of $m^* = \cos\theta^*$. The estimate is straight–forward: Since $|m^*|$ is w–periodic, we have

$$\begin{aligned} |m_n^*| &\leq \frac{1}{(2w)^{\frac{1}{2}}} \int_{-w}^{w} |m^*(x)|\,dx \\ &= (\frac{2}{w})^{\frac{1}{2}} \int_{-\frac{w}{2}}^{\frac{w}{2}} |m^*(x)|\,dx \\ &\overset{(i)}{=} (\frac{2}{w})^{\frac{1}{2}} \int_{-\frac{w}{2}}^{\frac{w}{2}} m^*(x)\,dx \\ &\overset{(ii)}{\leq} (\frac{2}{w})^{\frac{1}{2}}\,\pi. \end{aligned}$$

The leading order scaling for the Fourier coefficients corresponding to

$$n \quad \text{odd}, \qquad |n| \ll w \tag{105}$$

is obtained as follows. Since for odd n, $e^{i\,\pi\,n\,\frac{x}{w}}\,m^*(x)$ is w–periodic, we have

$$\begin{aligned} m_n^* &= (\frac{2}{w})^{\frac{1}{2}} \int_{\frac{w}{2}}^{\frac{w}{2}} e^{i\,\pi\,n\,\frac{x}{w}}\,m^*(x)\,dx \\ &= (\frac{2}{w})^{\frac{1}{2}} \left\{ \int_{-\frac{w}{2}}^{\frac{w}{2}} m^*(x)\,dx + \int_{-\frac{w}{2}}^{\frac{w}{2}} (e^{i\,\pi\,n\,\frac{x}{w}} - 1)\,m^*(x)\,dx \right\}. \end{aligned}$$

According to ii) we have

$$\int_{-\frac{w}{2}}^{\frac{w}{2}} m^*(x)\,dx \approx \pi.$$

According to i) and ii) we have

$$\begin{aligned} \left| \int_{-\frac{w}{2}}^{\frac{w}{2}} (e^{i\,\pi\,n\,\frac{x}{w}} - 1)\,m^*(x)\,dx \right| &\leq \int_{-\frac{w}{2}}^{\frac{w}{2}} |\pi\,n\,\frac{x}{w}|\,|m^*(x)|\,dx \\ &\overset{(i)}{=} \pi\,\frac{|n|}{w} \int_{-\frac{w}{2}}^{\frac{w}{2}} |x|\,m^*(x)\,dx \\ &\overset{(ii)}{\lesssim} \frac{|n|}{w} \overset{(105)}{\ll} 1. \end{aligned}$$

The argument for iv) is easy: According to $\theta^*(0) = 0$ and (39) we have

$$\frac{d\theta^*}{dx}(0) = (1+\epsilon^2)^{\frac{1}{2}} \overset{(103)}{\approx} 1.$$

From this and $\theta^*(0) = 0$ we obtain

$$\begin{aligned} m^*(0) &= \cos\theta^*(0) = 1, \\ \frac{dm^*}{dx}(0) &= -\sin\theta^*(0)\,\frac{d\theta^*}{dx}(0) = 0, \\ \frac{d^2m^*}{dx^2}(0) &= -\cos\theta^*(0)\left(\frac{d\theta^*}{dx}(0)\right)^2 - \sin\theta^*(0)\,\frac{d^2\theta^*}{dx^2}(0) = -\left(\frac{d\theta^*}{dx}(0)\right)^2 \approx -1. \end{aligned}$$

Since $\epsilon \ll 1$ is a regular perturbation of the equation (39) for θ^*, this implies that

$$\left.\begin{array}{rcl} 1-m^* & \approx & \frac{1}{2}\,x^2 \\ \frac{dm^*}{dx} & \approx & x \end{array}\right\} \quad \text{for} \quad |x| \ll 1$$

uniformly in $w \gg 1$.

We finally address v): From (101) and (102) we conclude for $0 \le x \le \frac{w}{2}$

$$\begin{aligned} \frac{w}{2}-x \;=\; \int_{\theta^*(x)}^{\frac{\pi}{2}} \frac{1}{(\cos^2\theta+\epsilon^2)^{\frac{1}{2}}}\,d\theta \;&\ge\; \int_{\theta^*(x)}^{\frac{\pi}{2}} \frac{1}{((\frac{\pi}{2}-\theta)^2+\epsilon^2)^{\frac{1}{2}}}\,d\theta \\ &\ge\; \int_{\theta^*(x)}^{\frac{\pi}{2}} \frac{1}{(\frac{\pi}{2}-\theta)+\epsilon}\,d\theta \\ &=\; \ln\left[\frac{1}{\epsilon}\,(\frac{\pi}{2}-\theta^*(x))+1\right], \end{aligned}$$

so that

$$\frac{1}{\epsilon}\,(\frac{\pi}{2}-\theta^*(x)) \;\le\; \exp(\frac{w}{2}-x).$$

According to (103), this implies

$$\frac{\pi}{2}-\theta^*(x) \;\lesssim\; \exp(-x). \tag{106}$$

On the other hand, according to (104),

$$\frac{\pi}{2}-\theta^*(x) \;\ge\; 0 \quad \text{for} \quad 0 \le x \le \frac{w}{2}.$$

Hence

$$0 \;\le\; \frac{\pi}{2}-\theta^*(x) \overset{(106)}{\lesssim} \exp(-x) \ll 1 \quad \text{for} \quad 1 \ll x \le \frac{w}{2}.$$

Hence $\theta^* \approx \frac{\pi}{2}$. Since $\cos\theta \approx \frac{\pi}{2}-\theta$ for $\theta \approx \frac{\pi}{2}$, we have

$$m^*(x) \;=\; \cos\theta^*(x) \;\approx\; \frac{\pi}{2}-\theta^*(x) \overset{(106)}{\lesssim} \exp(-x).$$

The claim of v) follows from the symmetry $m^*(-x) = m^*(x)$, which can be read off (101). □

Proof of Lemma 10:
We observe that

$$g(z) \;=\; \frac{\sinh(z)}{z\exp(z)} \;=\; \frac{1}{2\,z}\,(1-\exp(-2z)) \;\le\; \left\{\begin{array}{c} 1 \\ \frac{1}{2\,z} \end{array}\right\}.$$

Hence we obtain the estimate

$$\begin{aligned}
&\sum_n g\left(\frac{\pi\,|n|\,t}{2\,w}\right)\,|m_n^*|^2 \\
&\quad\lesssim \sum_{|n|\le\frac{w}{t}} |m_n^*|^2 \;+\; \frac{w}{t}\sum_{|n|>\frac{w}{t}}\frac{1}{|n|}\,|m_n^*|^2 \\
&\quad= \sum_{|n|\le\frac{w}{t}} |m_n^*|^2 \;+\; \frac{w}{t}\sum_{\frac{w}{t}<|n|\le w}\frac{1}{|n|}\,|m_n^*|^2 \;+\; \frac{w}{t}\sum_{|n|>w}\frac{1}{|n|}\,|m_n^*|^2.
\end{aligned}$$

We consider the three terms on the r. h. s. separately: According to Lemma 9 iii) we have

$$\sum_{|n|\le\frac{w}{t}} |m_n^*|^2 \;\lesssim\; \frac{1}{w}\sum_{|n|\le\frac{w}{t}} 1 \;\lesssim\; \frac{1}{t} \;\ll\; \frac{1}{t}\ln\,t$$

and

$$\frac{w}{t}\sum_{\frac{w}{t}<|n|\le w}\frac{1}{|n|}\,|m_n^*|^2 \;\lesssim\; \frac{1}{t}\sum_{\frac{w}{t}<|n|\le w}\frac{1}{|n|} \;\lesssim\; \frac{1}{t}\,\ln t.$$

For the last term we observe

$$\begin{aligned}
\frac{w}{t}\sum_{|n|>w}\frac{1}{|n|}\,|m_n^*|^2 \;&\lesssim\; \frac{1}{t}\sum_{|n|>w}\left(\frac{\pi\,|n|}{w}\right)^2\,|m_n^*|^2 \\
&\le\; \frac{1}{t}\int_{-w}^{w}(\frac{dm^*}{dx})^2\,dx \\
&\le\; \frac{1}{t}\int_{-w}^{w}(\frac{d\theta^*}{dx})^2\,dx \\
&\lesssim\; \frac{1}{t} \;\ll\; \frac{1}{t}\,\ln t.
\end{aligned}$$

□

Proof of Lemma 11:
We observe that also $m^* \;=\; \cos\theta^*$ obeys the symmetry

$$m^*(x+w) \;=\; -m^*(x).$$

On the level of Fourier coefficients, real functions with this symmetry are characterized by

$$\bar{\zeta_n} \;=\; \zeta_{-n} \qquad \text{and} \qquad \zeta_n \;=\; 0 \quad \text{for } n \text{ even}. \tag{107}$$

Minimizing the functional

$$\sum_n f\left(\frac{\pi\,|n|\,t}{2\,w}\right)\,|\zeta_n|^2 \;-\; 2\sum_n g\left(\frac{\pi\,|n|\,t}{2\,w}\right)\,\mathrm{Re}(\zeta_n\,\overline{m_n^*})$$

among all Fourier coefficients with (107), we obtain the Euler–Lagrange equation

$$f\left(\frac{\pi\,|n|\,t}{2\,w}\right)\,\zeta_n \;=\; g\left(\frac{\pi\,|n|\,t}{2\,w}\right)\,m_n^*,$$

since also m_n^* satisfies (107). Hence we obtain the following expression for the minimum

$$-\sum_n (g^2/f)\left(\frac{\pi\,|n|\,t}{2\,w}\right)\,|m_n^*|^2.$$

According to Lemma 9 iii),

$$\sum_n (g^2/f)\left(\frac{\pi\,|n|\,t}{2\,w}\right)\,|m_n^*|^2 \;\le\; \frac{2\,\pi^2}{w}\sum_{n\,odd}(g^2/f)\left(\frac{\pi\,|n|\,t}{2\,w}\right).$$

We observe that as a consequence of (8),

$$(g^2/f)(z) \;\approx\; \left\{\begin{array}{ll} \dfrac{1}{z} & \text{for} \quad z \;\ll\; 1 \\ \dfrac{1}{4\,z^2} & \text{for} \quad z \;\gg\; 1 \end{array}\right\},$$

so that the integral $\int_0^\infty (g^2/f)(z)dz$ diverges logarithmically at $z=0$. Since $\frac{t}{w} \;\ll\; 1$, we therefore have

$$\sum_{n\,odd}(g^2/f)\left(\frac{\pi\,|n|\,t}{2\,w}\right) \;\approx\; \frac{2\,w}{\pi\,t}\,\ln\frac{w}{t} \;\overset{w\gg t\gg 1}{\approx}\; \frac{2\,w}{\pi\,t}\,\ln w.$$

□

Proof of Lemma 12:
The symmetries (99) follow from the following symmetries

$$\bar{\zeta}_n \;=\; \zeta_{-n} \;=\; \zeta_n \qquad \text{and} \qquad \zeta_n \;=\; 0 \;\text{ for even } n$$

of the Fourier coefficients. We start by arguing that

$$\lambda \;\approx\; 3\sqrt{8} \;\sim\; 1. \tag{108}$$

Indeed, λ is defined via

$$\lambda \sum_{\substack{|n|>w \\ n\,odd}} \frac{w^3\,\ln w}{|n|^4} \;=\; \sum_{\substack{|n|\le\frac{w}{t} \\ n\,odd}} \frac{\sqrt{8}}{|n|}.$$

The leading order (108) of λ now follows from

$$\sum_{\substack{|n|>w \\ n\,odd}} \frac{1}{|n|^4} \;\overset{w\gg 1}{\approx}\; \int_w^\infty \frac{1}{z^4}\,dz \;=\; \frac{1}{3}\,\frac{1}{w^3},$$

$$\sum_{\substack{|n|\le\frac{w}{t} \\ n\,odd}} \frac{1}{|n|} \;\overset{w\gg t}{\approx}\; \int_1^{\frac{w}{t}} \frac{1}{z}\,dz \;=\; \ln\frac{w}{t} \;\overset{w\gg t\gg 1}{\approx}\; \ln w.$$

For the estimate itself, we shall establish

$$\frac{1}{2}\sum_{|n|\le\frac{w}{t}} f\left(\frac{\pi\,|n|\,t}{2\,w}\right)\,|\zeta_n|^2 \;\lessapprox\; 2\,\pi\,\frac{1}{t}\,\ln w, \tag{109}$$

$$\sum_{|n|\le\frac{w}{t}} g\left(\frac{\pi\,|n|\,t}{2\,w}\right)\,\mathrm{Re}(\zeta_n\,\bar{m}_n^*) \;\approx\; 4\,\pi\,\frac{1}{t}\,\ln w, \tag{110}$$

$$\sum_{|n|>w} f\left(\frac{\pi\,|n|\,t}{2\,w}\right)\,|\zeta_n|^2 \;\lesssim\; (\frac{1}{t}\,\ln w)^2, \tag{111}$$

$$\left|\sum_{|n|>w} g\left(\frac{\pi\,|n|\,t}{2\,w}\right)\,\mathrm{Re}(\zeta_n\,\bar{m}_n^*)\right| \;\lesssim\; \frac{1}{t^2}\,\ln w. \tag{112}$$

We observe that thanks to $\frac{1}{t}\,\ln w \;\ll\; 1$ and $t \;\gg\; 1$, the terms (111) and (112) are of higher order.

We start with (109). We observe

$$f(z) \;\le\; z \quad \text{for all } z, \tag{113}$$

which can be seen by writing

$$f(z) \;=\; 1-\frac{1}{2\,z}\,(1-\exp(-2\,z))$$

and using

$$\exp(-w) \;\le\; 1-w+\frac{1}{2}\,w^2 \quad \text{for all} \quad w \;\ge\; 0.$$

We now have

$$\begin{aligned}
\frac{1}{2}\sum_{|n|\le\frac{w}{t}} f\left(\frac{\pi\,|n|\,t}{2\,w}\right)\,|\zeta_n|^2 &\overset{(113)}{\le} \frac{1}{2}\sum_{|n|\le\frac{w}{t},n\,odd}\frac{\pi\,|n|\,t}{2\,w}\left(\frac{1}{t}\,\frac{(8\,w)^{\frac{1}{2}}}{|n|}\right)^2\\
&= \frac{2\,\pi}{t}\sum_{|n|\le\frac{w}{t},n\,odd}\frac{1}{|n|}\\
&\overset{w\gg t}{\approx} \frac{2\,\pi}{t}\,\ln\frac{w}{t}\\
&\overset{w\gg t\gg 1}{\approx} \frac{2\,\pi}{t}\,\ln w.
\end{aligned}$$

We now address (110). Since $t \;\gg\; 1$ and thus $\frac{w}{t} \ll w$, we have according to Lemma 9 iii)

$$m_n^* \;\approx\; (\frac{2}{w})^{\frac{1}{2}}\,\pi \quad \text{for all} \quad |n| \;\le\; \frac{w}{t}, \quad n \text{ odd}.$$

Therefore

$$\begin{aligned}
\sum_{|n|\le\frac{w}{t}} g\left(\frac{\pi\,|n|\,t}{2\,w}\right)\,\mathrm{Re}(\zeta_n\,\bar{m}_n^*) &\approx \sum_{|n|\le\frac{w}{t},n\,odd} g\left(\frac{\pi\,|n|\,t}{2\,w}\right)\,\frac{1}{t}\,\frac{(8\,w)^{\frac{1}{2}}}{|n|}\,(\frac{2}{w})^{\frac{1}{2}}\,\pi\\
&= \frac{2\,\pi^2}{w}\sum_{|n|\le\frac{w}{t},n\,odd} g\left(\frac{\pi\,|n|\,t}{2\,w}\right)\,\frac{2\,w}{\pi\,|n|\,t}.
\end{aligned}$$

Since

$$g(z)\,\frac{1}{z} \;\approx\; \frac{1}{z} \quad \text{for} \quad z \ll 1,$$

the integral $\int_0^\infty g(z)\,\frac{1}{z}\,dz$ diverges logarithmically at $z = 0$. Therefore we obtain because of $\frac{t}{w} \ll 1$:

$$\begin{aligned}\sum_{|n|\leq \frac{w}{t}, n \text{ odd}} g\left(\frac{\pi\, t\, |n|}{2\, w}\right)\, \frac{2\, w}{\pi\, |n|\, t} \quad &\approx \quad \frac{2\, w}{\pi\, t}\, \ln \frac{w}{t} \\ &\overset{w \gg t \gg 1}{\approx} \quad \frac{2\, w}{\pi\, t}\, \ln w.\end{aligned}$$

Hence as desired

$$\sum_{|n|\leq \frac{w}{t}} g\left(\frac{\pi\, |n|\, t}{2\, w}\right)\, \mathrm{Re}(\zeta_n\, \bar{m}_n^*) \;\approx\; \frac{4\, \pi}{t}\, \ln w.$$

We now estimate the term (111):

$$\begin{aligned}\sum_{|n|>w} f\left(\frac{\pi\, |n|\, t}{2\, w}\right)\, |\zeta_n|^2 \quad &\overset{(108)}{\lesssim} \quad \frac{w^7\, \ln^2 w}{t^2}\, \sum_{|n|>w} f\left(\frac{\pi\, |n|\, t}{2\, w}\right)\, \frac{1}{|n|^8} \\ &\overset{f \leq 1}{\lesssim} \quad \frac{w^7\, \ln^2 w}{t^2}\, \sum_{|n|>w} \frac{1}{|n|^8} \\ &\overset{w \gg 1}{\lesssim} \quad \frac{w^7\, \ln^2 w}{t^2}\, \int_w^\infty \frac{1}{z^8}\, dz \\ &\lesssim \quad (\frac{\ln w}{t})^2.\end{aligned}$$

We finally address (112). We use

$$g(z) \;\leq\; \frac{1}{z} \quad \text{for all } z \tag{114}$$

and Lemma 9 iii) in form of

$$|m_n^*| \;\lesssim\; \frac{1}{w^{\frac{1}{2}}}. \tag{115}$$

We have

$$\begin{aligned}&\left|\sum_{|n|>w} g\left(\frac{\pi\, |n|\, t}{2\, w}\right)\, \mathrm{Re}(\zeta_n\, m_n^*)\right| \\ &\quad \overset{(108)}{\lesssim} \quad \frac{w^{\frac{7}{2}}\, \ln w}{t}\, \sum_{|n|>w} g\left(\frac{\pi\, |n|\, t}{2\, w}\right)\, \frac{1}{|n|^4}\, |m_n^*| \\ &\quad \overset{(114),(115)}{\lesssim} \quad \frac{w^4\, \ln w}{t^2}\, \sum_{|n|>w} \frac{1}{|n|^5} \\ &\quad \overset{w \gg 1}{\lesssim} \quad \frac{w^4\, \ln w}{t^2}\, \int_w^\infty \frac{1}{z^5}\, dz \\ &\quad \lesssim \quad \frac{\ln w}{t^2}.\end{aligned}$$

□

PROOF OF LEMMA 13:
By definition of λ, we have

$$\zeta(0) \;=\; \frac{1}{(2w)^{\frac{1}{2}}} \sum_n \zeta_n \;=\; 0.$$

Furthermore, $\frac{d\zeta}{dx}(0) \;=\; 0$ follows from the symmetry

$$\zeta(-x) \;=\; \zeta(x).$$

This establishes i).

We now address ii). In terms of the Fourier coefficients, ii) follows from

$$\frac{1}{(2\,w)^{\frac{1}{2}}} \sum_n |\zeta_n| \;+\; \frac{1}{(2\,w)^{\frac{1}{2}}} \sum_n \frac{\pi\,|n|}{w}\,|\zeta_n| \;+\; \frac{1}{(2\,w)^{\frac{1}{2}}} \sum_n \left(\frac{\pi\,|n|}{w}\right)^2 |\zeta_n| \;\lesssim\; \frac{\ln w}{t},$$

which amounts to

$$\frac{1}{w^{\frac{1}{2}}} \sum_{|n|\leq w} |\zeta_n| \;\lesssim\; \frac{\ln w}{t} \quad \text{and} \quad \frac{1}{w^{\frac{1}{2}}} \sum_{|n|>w} \left(\frac{|n|}{w}\right)^2 |\zeta_n| \;\lesssim\; \frac{\ln w}{t}.$$

This is indeed the case:

$$\frac{1}{w^{\frac{1}{2}}} \sum_{|n|\leq w} |\zeta_n| \;\lesssim\; \frac{1}{t} \sum_{|n|\leq w} \frac{1}{|n|} \;\overset{w\gg 1}{\lesssim}\; \frac{\ln w}{t}$$

and

$$\begin{aligned} \frac{1}{w^{\frac{1}{2}}} \sum_{|n|>w} \left(\frac{|n|}{w}\right)^2 |\zeta_n| \quad &= \quad \frac{1}{w^{\frac{5}{2}}} \sum_{|n|>w} |n|^2\,|\zeta_n| \\ &\overset{(108)}{\lesssim} \quad \frac{w\,\ln w}{t} \sum_{|n|>w} \frac{1}{|n|^2} \\ &\overset{w\gg 1}{\lesssim} \quad \frac{\ln w}{t}. \end{aligned}$$

Part iii) follows from

$$\begin{aligned} \int_{-w}^{w} (\frac{d\zeta}{dx})^2\,dx \quad &= \quad \sum_n \left(\frac{\pi\,|n|}{w}\right)^2 |\zeta_n|^2 \\ &\overset{(108)}{\lesssim} \quad \frac{1}{t^2\,w} \sum_{|n|\leq \frac{w}{t}} 1 \;+\; \frac{w^5\,\ln^2 w}{t^2} \sum_{|n|>w} \frac{1}{|n|^6} \\ &\overset{w\gg 1}{\lesssim} \quad \frac{1}{t^3} \;+\; \left(\frac{\ln w}{t}\right)^2 \\ &\overset{w\gg t\gg 1}{\lesssim} \quad \left(\frac{\ln w}{t}\right)^2. \end{aligned}$$

We finally tackle iv). According to Lemma 9 iv)

$$\left\{ \begin{array}{ccc} 1-m^* & \approx & \frac{1}{2}\,x^2 \\ \frac{dm^*}{dx} & \approx & x \end{array} \right\} \quad \text{for} \quad |x| \ll 1. \tag{116}$$

According to parts i) and ii) of this lemma

$$\left. \begin{array}{ccc} |\zeta| & \lesssim & \frac{\ln w}{t}\,x^2 \\ |\frac{d\zeta}{dx}| & \lesssim & \frac{\ln w}{t}\,x \end{array} \right\}. \tag{117}$$

Since $\ln w \ll t$, this implies in particular

$$\left. \begin{array}{ccc} 1-m & \approx & \frac{1}{2}\,x^2 \\ \frac{dm}{dx} & \approx & x \end{array} \right\} \quad \text{for} \quad |x| \ll 1. \tag{118}$$

We conclude from (116), (117) & (118):

$$\begin{aligned} &\max\left\{\frac{1}{1-m^2}\,,\,\frac{1}{1-(m^*)^2}\right\}\,(\frac{d\zeta}{dx})^2 \\ &\quad + \max\left\{\frac{1}{1-m^2}\,,\,\frac{1}{1-(m^*)^2}\right\}^3\,\max\left\{(\frac{dm}{dx})^2,(\frac{dm^*}{dx})^2\right\}\,\zeta^2 \\ &\lesssim\ (\frac{\ln w}{t})^2 \qquad \text{for} \quad |x| \ll 1. \end{aligned} \tag{119}$$

This deals with the small $|x|$–values.

For the large $|x|$-values we observe that according to Lemma 9 i) and v)

$$|m^*| \ \lesssim\ \exp(-|x|) \quad \text{for} \quad 1 \ll |x| \ \leq\ \frac{w}{2}.$$

On the other hand, we obtain from (116) and the monotonicity (41) that also

$$|m^*| \ \leq\ c_0 \ <\ 1 \quad \text{for} \quad |x| \ \sim\ 1.$$

Together with part ii) of this lemma, i. e.

$$|\zeta| \ \lesssim\ \frac{\ln w}{t} \ \ll\ 1,$$

we conclude

$$\max\left\{\frac{1}{1-m^2},\frac{1}{1-(m^*)^2}\right\} \ \lesssim\ 1 \quad \text{for} \quad 1 \ \lesssim\ |x| \ \leq\ \frac{w}{2}.$$

Thus

$$\begin{aligned}
&\max\left\{\frac{1}{1-m^2}\,,\,\frac{1}{1-(m^*)^2}\right\}\,(\frac{d\zeta}{dx})^2\\
&\quad+\max\left\{\frac{1}{1-m^2}\,,\,\frac{1}{1-(m^*)^2}\right\}^3\,\max\left\{(\frac{dm}{dx})^2,(\frac{dm^*}{dx})^2\right\}\,\zeta^2\\
&\quad\lesssim\;(\frac{d\zeta}{dx})^2+(\frac{\ln w}{t})^2\max\left\{(\frac{dm}{dx})^2,(\frac{dm^*}{dx})^2\right\}\\
&\quad\overset{\ln w\ll t}{\lesssim}\;(\frac{d\zeta}{dx})^2+(\frac{\ln w}{t})^2\,(\frac{dm^*}{dx})^2\\
&\quad\leq\;(\frac{d\zeta}{dx})^2+(\frac{\ln w}{t})^2\,(\frac{d\theta^*}{dx})^2\quad\text{for}\quad 1\;\lesssim\;|x|\;\leq\;\frac{w}{2}.
\end{aligned}\tag{120}$$

From (119) and (120) we obtain

$$\begin{aligned}
&\int_{-\frac{w}{2}}^{\frac{w}{2}}\Big\{\max\left\{\frac{1}{1-m^2}\,,\,\frac{1}{1-(m^*)^2}\right\}\,(\frac{d\zeta}{dx})^2\\
&\quad+\max\left\{\frac{1}{1-m^2}\,,\,\frac{1}{1-(m^*)^2}\right\}^3\,\max\left\{(\frac{dm}{dx})^2,(\frac{dm^*}{dx})^2\right\}\,\zeta^2\Big\}\,dx\\
&\lesssim\;(\frac{\ln w}{t})^2\,\left(1+\int_{-\frac{w}{2}}^{\frac{w}{2}}(\frac{d\theta^*}{dx})^2\,dx\right)\;+\;\int_{-\frac{w}{2}}^{\frac{w}{2}}(\frac{d\zeta}{dx})^2\,dx.
\end{aligned}$$

We now conclude by evoking Proposition 1, which yields $\int_{-\frac{w}{2}}^{\frac{w}{2}}(\frac{d\theta^*}{dx})^2\,dx\;\lesssim\;1$, and part iii) of this lemma. □

6 Acknowledgments

ADS & SM were partially supported by the TMR network FMRX–CT98–0229. ADS & SM and FO acknowledge partial support by the Deutsche Forschungsgemeinschaft through SPP 1095 resp. SFB 611. RVK thanks the National Science Foundation for partial support. FO would like to thank Weinan E for stimulating discussions and the Morningside Center of Mathematical Sciences in Beijing for its hospitality. Thanks also to Michael Westdickenberg and Ruben Cantero for pointing out some simplifications.

References

[1] F. Alouges, T. Rivére, S. Serfaty, Néel and cross-tie wall energies for planar micromagnetic configurations, submitted to COCV

[2] A. DeSimone, R. V. Kohn, S. Müller, F. Otto, Magnetic microstructures — a paradigm of multiscale problem, in *Proceedings of the ICIAM 1999*, J. M. Ball & J. C. R. Hunt eds. , pp. 175 – 190 (2000)

[3] A. DeSimone, R.V. Kohn, S. Müller, F. Otto and R. Schäfer, Low energy domain patterns in soft ferromagnetic films, *J. Magnetism Magn. Mat.*, in press (2002).

[4] C. Garcia–Cervera, Magnetic domains and magnetic domain walls, Ph–D thesis, New York University (1999)

[5] A. Hubert, Interaction of domain walls in thin magnetic films, *Czech. J. Phys. B* **21**, pp. 532 – 536 (1971).

[6] A. Holz, A. Hubert, Wandstrukturen in dünnen magnetischen Schichten, *Z. angew. Phys.* **26** (2), pp. 145 – 152 (1969).

[7] A. Hubert, R. Schäfer, *Magnetic domains*, Springer, (1998).

[8] C. Melcher, The logarithmic tail of Néel walls in thin films, submitted to *Arch. Rat. Mech. Anal.*.

[9] S. Middelhoek, Domain walls in thin Ni–Fe Films, *J. Appl. Phys.* **34** (4), pp. 1054 – 1059 (1963)

[10] H. Riedel, A. Seeger, Micromagnetic treatment of Néel walls, *Phys. Stat. Sol. (b)* **46**, pp. 377 – 384 (1971).